

Model Explanations with Differential Privacy

Neel Patel, Reza Shokri, Yair Zick
National University of Singapore (NUS)
{neel, reza, zick}@comp.nus.edu.sg

Abstract

Black-box machine learning models are used in critical decision-making domains, giving rise to several calls for more *algorithmic transparency*. The drawback is that model explanations can leak information about the training data and the explanation data used to generate them, thus undermining *data privacy*. To address this issue, we propose differentially private algorithms to construct feature-based model explanations. We design an adaptive differentially private gradient descent algorithm, that finds the minimal privacy budget required to produce accurate explanations. It reduces the overall privacy loss on explanation data, by adaptively reusing past differentially private explanations. It also amplifies the privacy guarantees with respect to the training data. We evaluate the implications of differentially private models and our privacy mechanisms on the quality of model explanations.

1 Introduction

Machine learning models are currently applied in a variety of high-stakes domains, e.g. providing predictive healthcare analytics, assessing insurance policies, and making credit decisions. These domains require high prediction accuracy over high-dimensional data; as a result, they adopt increasingly complex architectures, making them harder to interpret. What makes the problem even more challenging is that these models are usually used as *black-box algorithms*: they only output a decision, without providing detailed information on its intermediate computations. Growing mistrust of black-box algorithms in high-stakes domains resulted in a widespread call for *algorithmic transparency* [17, 20]. This term broadly refers to methods that offer additional information about the underlying algorithmic decision-making process. In this work, we focus on model-agnostic feature based explanations as in [6, 11, 13, 21, 27, 33]. Model-agnostic methods often use a dataset labeled by the black-box model to generate model explanations, referred to as the *explanation dataset*. This dataset is often just a subset of the training data, or sampled from the same distribution.

The problem is that offering additional information can result in significant *data privacy risks*, by leaking sensitive information about the underlying explanation and training data, which can be exploited by inference attacks [29]. Some feature-based model explanations directly depend on model parameters [3, 5, 31, 32, 35], which even further increases their privacy vulnerabilities with respect to white-box inference attacks [25]. As a related issue, model explanations can also magnify the risks of model reconstruction attacks [24], which are however not the focus of this paper. Thus far, there has been little work on modeling the relation between algorithmic *transparency and privacy* [13, 18, 29], and on designing *model explanations that protect data privacy*. The destructive impact of randomized privacy mechanisms on the fidelity of model explanations is also not studied.

1.1 Our Contributions

We propose provably sound, model-agnostic, and differentially private algorithms for computing model explanations that protect the sensitive information in the *explanation* and *training datasets*. Our explanations are sound in the sense that they are provably similar to some standard model explanations, such as LIME [27]. Our methodology can be adapted to any explanation method that relies on generating accurate local models around the data point one tries to explain.

We first design a baseline interactive mechanism that outputs feature-based model explanations, while guaranteeing differential privacy for each query. Building upon this baseline, we design our main algorithm: an *adaptive differential privacy mechanism for model explanations*. The main challenge, which we resolve in this approach, is to optimize the composed privacy loss of the model explanation over all queries, while maintaining low explanation error. The adaptive algorithm utilizes previously released DP explanations effectively, significantly reducing privacy spending on new model explanation queries. We achieve this by selecting a better initialization point for the our underlying gradient descent algorithm using past queries. We also improve upon bounds in [28] on the convergence of the DP gradient descent method (under a minor assumption), offering faster initialization-dependent convergence rates. We further show that when we approach the optimal point, the DP gradient descent algorithm oscillates around the optimal point, spending a significant chunk of the privacy budget while obtaining only a negligible expected utility. This insight leads to an *enhanced adaptive algorithm* which offers far better privacy savings at only a minor loss in accuracy. Finally, we propose a *non-interactive* differential privacy algorithm which generates explanations without spending any further privacy budget.

Our algorithms bound the (differential) privacy loss with respect to explanation data. Privacy protection of the training data is normally done during model training, or via differentially private prediction algorithms. However, we show that our mechanism, which uses the underlying model as a black-box, can also moderately amplify the privacy protection of the training data. As mentioned previously, protecting the privacy of sensitive data must be done in tandem with *preserving explanation quality*: this is crucial as the randomness in differential privacy mechanisms might reduce explanation fidelity. Ensuring that our mechanisms preserve explanation quality requires careful analysis of the underlying gradient descent mechanism: we determine the number of iterations required to minimize the privacy budget spending required for an explanation query, hence maximizing the overall explanation quality. When protecting data using differentially private models, the randomness in the decision boundaries of differentially private models decreases the convergence speed of our approximation algorithms, which results in spending more privacy budget. This is demonstrated in our empirical results: stronger privacy requirements for the underlying model degrade explanation quality.

1.2 Related Work

Model explanations are vulnerable to membership inference attacks that can infer if a data point is part of the model’s training set [29]. A recent work [18] studies the construction of differentially private and interpretable *predictions* — rather than explanations — for neural networks. But, it does not offer any bounds on the utility loss due to privacy. An earlier work presents QII [13] that designs an interactive differentially private mechanism to protect the explanation dataset. However, repeated queries result in an unacceptable cumulative information leakage and a loose privacy guarantee. It also does not provide any privacy analysis for the training dataset.

Table 1: Table of Notations

Notation	Description
\mathcal{X}	explanation dataset
\mathcal{T}	training dataset
m	size of the dataset \mathcal{X}
n	dimension of the dataset \mathcal{X}
$f(\cdot)$	black-box model
$(\hat{\epsilon}, \hat{\delta})$	privacy parameters differentially private model
(ϵ, δ)	privacy parameters for explanation for explanation dataset
$\phi^{Priv}(\cdot)$	private explanation
$\mathcal{C}_{p,k}$	convex set of possible explanations $\{\phi : \ \phi\ _p \leq k\}$
$\alpha : \mathbb{R}^+ \rightarrow \mathbb{R}^+$	weight function
$\mathcal{L}(\cdot)$	loss function
$\phi^*(\cdot)$	optimal solution of the loss function $\mathcal{L}(\cdot)$
$\mathcal{F}(c, \vec{z})$	class of weight functions with bounded sensitivity of c
$\mathcal{E}(\phi^{Priv})$	utility loss of the private explanation ϕ^{Priv}
$(\epsilon_{min}, \delta_{min})$	minimum privacy requirement for each query
ϵ_{ite}	privacy spending at each gradient descent iteration
σ_{min}	variance required by the Gaussian mechanism
\mathcal{H}	history consist of explained queries in past
\mathcal{X}'	proxy explanation dataset for non-interactive phase
γ	amplification of the training privacy

2 Problem Statement

Consider a black-box decision-making machine learning model $f : \mathbb{R}^n \rightarrow \mathcal{R}$ trained on the *training dataset* \mathcal{T} . The model returns the predicted label, and provides no more information about its decision. Our goal is to generate a *model explanation* $\phi(\vec{z}, \mathcal{X}, f(\mathcal{X}))$, whose input is a *point of interest* \vec{z} , an *explanation dataset* $\mathcal{X} = \{\vec{x}_1, \dots, \vec{x}_m\} \subset \mathbb{R}^n$ (used to generate the explanation), and the output of f on \mathcal{X} . Model explanation algorithms can also use additional information: this can be a prior over the data [6], access to model queries [1, 13, 27], knowledge about the model hypothesis class [2, 31, 35], or access to the source code [12]. Table 1 summarizes our notations. We focus on *feature-based* model explanations: $\phi(\vec{z})$ is a vector in \mathbb{R}^n , where $\phi_i(\vec{z})$ measures the effect that the i -th feature has on the predicted label $f(\vec{z})$.

Existing explanation algorithms assume some degree of access to data labeled by f . Access to the relevant data for generating explanations is crucial: when having only black-box access to the model, information about its behavior over data is essentially the only available source one can use to generate explanations. In addition, it is crucial that \mathcal{X} is sampled from the same distribution as the data used to train f ; otherwise, one runs the risk of generating explanations that are inappropriate for the model’s actual behavior on the data that it was given (see discussion in [13]). Indeed, using the training set to generate explanations is standard practice [17].

2.1 Model Explanations

Feature based explanations are often local model approximations in a region around the point of interest \vec{z} [27, 33, 32, 34]. Our objective is to find a linear function ϕ , centered at a point of interest \vec{z} , that minimizes the *local empirical model error* over the explanation dataset \mathcal{X} . We define the *empirical local loss* $\mathcal{L}(\phi, \vec{z}, \mathcal{X}, f)$ of a linear function ϕ , over \mathcal{X} labeled by f , as

$$\mathcal{L}(\phi, \vec{z}, \mathcal{X}, f) \triangleq \frac{1}{|\mathcal{X}|} \sum_{\vec{x} \in \mathcal{X}} \alpha(\|\vec{x} - \vec{z}\|) (\phi^\top \cdot (\vec{x} - \vec{z}) - f(\vec{x}))^2, \quad (1)$$

where, $\alpha : \mathbb{R}_+ \rightarrow \mathbb{R}_+$ is a weight function. We find a local explanation within some region \mathcal{C} that minimizes $\mathcal{L}(\phi, \vec{z}, \mathcal{X}, f)$. We assume \mathcal{C} to be a bounded convex set; more concretely, we set \mathcal{C} to $\mathcal{C}_{p,k} = \{\phi : \|\phi\|_p \leq k\}$. An *optimal* model explanation is thus one that minimizes loss around the point of interest.

$$\phi^*(\vec{z}) = \arg \min_{\phi \in \mathcal{C}} \mathcal{L}(\phi, \vec{z}, \mathcal{X}, f) \quad (2)$$

The weight function α is a decreasing function in $\|\vec{z} - \vec{x}\|$. In other words, ϕ is a *local explanation*, rewarded for correctly classifying points closer to \vec{z} . For example, in the LIME framework, α takes a value of 0 for any points $\vec{x} \in \mathcal{X}$ that are more than a certain distance away from the point of interest \vec{z} . Our framework generalizes LIME and other local optimization-based model explanations.

2.2 Evaluation Metrics

We assume an *adversary* queries the model f with a sequence of data points, requesting explanations for the model’s decisions over them. Given the obtained explanations, the adversary can reconstruct sensitive information about the explanation data \mathcal{X} , and the training data \mathcal{T} . Our objective is to design a differentially private algorithm that can provably *protect private data against inference attacks*, and provides accurate explanations. We evaluate our explanation models based on two key performance metrics: their differential *privacy loss*, and their *utility loss* in comparison to the *optimal explanation*, as described in Eq. (2).

Following the definition of *differential privacy* (DP) [15], a model explanation $\phi(\cdot)$ is (ϵ, δ) -differentially private if for any sequence of queries (points of interest) $\vec{z}_1, \vec{z}_2, \dots, \vec{z}_k$, for any two neighboring explanation datasets \mathcal{X} and \mathcal{X}' — i.e. datasets that differ by the omission of a single point — and any explanations $S_i \subseteq \mathbb{R}^n$, we have

$$\Pr[\phi_1 \in S_1, \phi_2 \in S_2, \dots, \phi_k \in S_k] \leq e^\epsilon \cdot \Pr[\phi'_1 \in S_1, \phi'_2 \in S_2, \dots, \phi'_k \in S_k] + \delta, \quad (3)$$

where, $\phi_i = \phi(\vec{z}_i, \mathcal{X}, f(\mathcal{X}))$, and $\phi'_i = \phi(\vec{z}_i, \mathcal{X}', f(\mathcal{X}'))$. We similarly define guarantees for two neighboring training datasets \mathcal{T} and \mathcal{T}' . This guarantees ensures that the adversary cannot accumulate enough information from their queries to reconstruct data records in the explanation set or training set, up to the protection level determined by privacy loss parameters for both datasets ϵ and δ respectively.

Our main focus is to protect the sensitive information about the explanation dataset \mathcal{X} , in Section 5, we show that our private explanations are differentially private w.r.t. *training dataset* as well.

Algorithm 1: Interactive DP Model Explanation

Input: POI $\vec{z} \in \mathbb{R}^n$, explanation dataset \mathcal{X} , DP parameters $\epsilon > 0, \delta > 0$, weight function $\alpha(\|\vec{x} - \vec{z}\|) \in \mathcal{F}(1, \vec{z})$, learning rate function $\eta(t) \in \mathbb{R}_+$, and the number of GD iterations T .

Output: ϕ^{Priv}

```
1: Set the parameter for the Gaussian mechanism  $\sigma \leftarrow \frac{1}{m\epsilon} \sqrt{16T \log(e + \frac{\sqrt{T}\epsilon}{\delta}) \log \frac{T}{\delta}}$ ;  
2: Initialize  $\phi$  with an arbitrary vector in  $\mathcal{C}_{2,1}$ ;  
3: return DPGD-Explain( $\phi, \sigma, T$ );  
4: Procedure DPGD-Explain( $\phi, \sigma, T$ )  
5:    $\phi^{\{1\}} \leftarrow \phi$   
6:   for  $t = 1, \dots, T - 1$  do  
7:      $\xi_t \leftarrow (\phi^{\{t\}} - \eta(t) [\nabla \mathcal{L}(\phi, \mathcal{X}) + \mathcal{N}(0, \sigma^2 \mathbf{I})])$   
8:      $\phi^{\{t+1\}} \leftarrow \arg \min_{\phi \in \mathcal{C}_{2,1}} \|\phi - \xi_t\|$   
9:   end  
10:  return  $\phi^{\{T\}}$ 
```

The *quality* of a model explanation is measured in terms the difference between its (expected) loss and the loss of the optimal explanation which is referred as approximation loss of explanation:

$$\mathcal{E}(\phi) = \mathbb{E}[\mathcal{L}(\phi, \vec{z}, \mathcal{X}, f)] - \mathcal{L}(\phi^*(\vec{z}), \vec{z}, \mathcal{X}, f), \quad (4)$$

In the following sections, we describe a variety of mechanisms computing differentially private model explanations. We start with a simple non-adaptive mechanism in Section 3, using it as a foundation for more complex adaptive mechanisms (Section 4). Finally, we show that our mechanisms offer privacy guarantees with respect to the training data as well (Section 5).

3 A Basic DP Mechanism for Model Explanation

We begin our exploration of differentially private model explanations with a simple approach: approximating each local model explanation in a differentially private manner. Algorithm 1 presents a gradient descent algorithm to solve (2) while satisfying differential privacy as in (3).

We compute a differentially private model explanation ϕ^{Priv} by optimizing (2) in the convex set $\mathcal{C}_{2,1}$. The gradient descent algorithm (the DPGD-Explain() procedure) uses the Gaussian mechanism in each iteration to guarantee differential privacy with respect to the explanation dataset. This is an interactive DP mechanism: for each query, we refer to the (explanation) dataset for computing the explanations.

The input to our proposed algorithm is the point of interest \vec{z} , and the explanation dataset \mathcal{X} labeled by the function f . It finds the solution in a feasible convex set \mathcal{C} (where we use $\mathcal{C}_{2,1}$), for a local loss function $\mathcal{L}(\cdot)$. Its output is a differentially private model explanation $\phi^{Priv}(\vec{z}, \mathcal{X}, \mathcal{C}, \mathcal{L})$, as we prove later in this section.

3.1 Sensitivity of the Loss Function

In order to design the differential privacy mechanism, with bounded privacy loss, we first need to bound the global sensitivity of the gradient of the loss function $\nabla \mathcal{L}(\cdot)$. The global sensitivity of $\nabla \mathcal{L}(\cdot)$ could be unbounded for many choices of $\alpha(\|\vec{x} - \vec{z}\|)$; for example, when $\alpha(\|\vec{x} - \vec{z}\|) = \frac{1}{\|\vec{x} - \vec{z}\|_2}$,

this weight function is non-increasing which is a required property for local model approximation. However, the sensitivity of $\nabla\mathcal{L}(\cdot)$ for this $\alpha(\cdot)$ is unbounded. Thus, we need to choose from a family of weight functions that result in a bounded sensitivity for $\nabla\mathcal{L}(\cdot)$, required by our DP mechanisms.

In Lemma 3.1 (whose proof is in the appendix), we characterize set of weight functions $\alpha(\|\vec{x} - \vec{z}\|_2)$ such that the sensitivity of $\nabla\mathcal{L}(\cdot)$ is bounded.

Lemma 3.1 (Conditions for Bounded Sensitivity for $\nabla\mathcal{L}(\cdot)$). *For all explanation dataset \mathcal{X} of size m , and all its neighboring datasets \mathcal{X}' , points of interest \vec{z} , and $\phi \in \mathcal{C}$, the sensitivity of the gradient of loss is bounded, $\|\nabla\mathcal{L}(\phi, \mathcal{X}) - \nabla\mathcal{L}(\phi, \mathcal{X}')\|_2 \leq (\frac{c}{m})$, iff $\alpha(\|\vec{x} - \vec{z}\|) \leq \frac{c}{2\|\vec{x} - \vec{z}\|_2(\|\vec{x} - \vec{z}\|_2 + 1)}$ for every $\vec{x}, \vec{z} \in \mathbb{R}^n$.*

Proof. See Appendix A □

Lemma 3.1 characterizes all weight functions $\alpha(\cdot)$ for which the sensitivity of the gradient $\nabla\mathcal{L}(\phi, \mathcal{X})$ is bounded. We define the family of desirable weight functions as:

$$\mathcal{F}(c, \vec{z}) = \left\{ \alpha(\cdot) : \begin{array}{l} \alpha(\cdot) \text{ is non-increasing and} \\ \forall \vec{x} \in \mathbb{R}^n, \alpha(\|\vec{x} - \vec{z}\|) \leq \frac{c}{2\|\vec{x} - \vec{z}\|(\|\vec{x} - \vec{z}\| + 1)} \end{array} \right\}.$$

Note that $\mathcal{F}(c, \vec{z})$ is non-empty as $\frac{c}{2\|\vec{x} - \vec{z}\|(\|\vec{x} - \vec{z}\| + 1)}$ belongs to the family. The choice of weight function governs how “local” the model approximation is around a point of interest. For example, $\alpha(\|\vec{x} - \vec{z}\|) = e^{-\|\vec{x} - \vec{z}\|^2}$ is in $\mathcal{F}(1, \vec{z})$ which exponentially decreases the weight of the data points according to their distance to the point of interest \vec{z} . This weight function is extremely local. Thus, it is useful when the explanation dataset \mathcal{X} is highly dense in different regions.

3.2 Privacy and Utility Guarantees

We bound the privacy and utility loss of model explanations produced by Algorithm 1. The data dependent quantity, in each iteration of Algorithm 1, is $\nabla\mathcal{L}(\phi, \mathcal{X})$. Given Lemma 3.1, we use the Gaussian mechanism to ensure that the update in each round is differentially private. Using the differential privacy composition theorem [19, Theorem-4.3], the output of algorithm 1 is (ϵ, δ) -differentially private. We show that the differentially private mechanism for model explanation offers good utility loss guarantees.

Theorem 3.2 (Bounded Utility Loss). *Algorithm 1 is (ϵ, δ) differentially private. Moreover, for given privacy parameters (ϵ, δ) , if $\text{DPGD-Explain}()$ runs for $T \leq \min\left(\frac{m^2\epsilon^2}{32n\log^2(e+1/\delta)}, \frac{1}{\delta}\right)$ iterations and outputs an explanation ϕ^{Priv} , then $\mathcal{E}(\phi^{Priv}) \in \mathcal{O}\left(\frac{\log T}{\sqrt{T}}\right)$. For $T = \frac{m^2\epsilon^2}{32n\log^2(e+1/\delta)}$, $\mathcal{E}(\phi^{Priv}) \in \mathcal{O}\left(\frac{\sqrt{n}\log m}{m\epsilon}\right)$.*

The bound in Theorem 3.2 is reasonable when the number of features is smaller than the size of the explanation dataset. Let ϕ^{Priv} be the output of the mechanism described in Theorem 3.2; while ϕ^{Priv} is differentially private in itself, its privacy loss accumulates as we make additional model explanation queries. Following the DP composition theorem [19], k independent (ϵ, δ) -private queries result in an $(\tilde{\epsilon}, k\delta + \tilde{\delta})$ -differentially private output for any $\tilde{\delta} \in (0, 1)$ and $\tilde{\epsilon} \in \mathcal{O}\left(\epsilon \times (ke^\epsilon + \sqrt{k \log(e + \epsilon\sqrt{k}/\tilde{\delta})})\right)$.

4 Adaptive Differential Privacy Mechanisms

The explanation algorithm described in Section 3 naively computes an explanation for a queried data point: it does not utilize any *previously released differentially private information*. When Algorithm 1 computes a model explanation, it releases information about the underlying black-box algorithm in a differentially private manner. This information can be used to generate an explanation for new queries more economically, resulting in less privacy spending. How can we utilize past information efficiently?

Let us define this problem more formally. Let $\vec{z}_1, \dots, \vec{z}_h$ be the sequence of queries previously explained in a differentially private manner, and their corresponding explanations: $\phi^{Priv}(\vec{z}_1), \dots, \phi^{Priv}(\vec{z}_h)$. When we receive a new query \vec{z}_{h+1} , our objective is to extract information from $(\vec{z}_1, \phi^{Priv}(\vec{z}_1)), \dots, (\vec{z}_h, \phi^{Priv}(\vec{z}_h))$ such that the new query \vec{z}_{h+1} requires less privacy budget, without compromising its explanation quality.

If the underlying black-box model behaves in a consistent manner within a local region, then model explanations in that local region should be consistent: this enables us to exploit previous queries from the same local region to explain the current query while spending less of the privacy budget. Moreover, if we can ensure that the `DPGD-Explain()` procedure converges faster by using past information, then also we can reduce the resultant privacy spending for the current query.

The above insights are used in our *Adaptive Private Interactive Explanation Protocol* (Algorithm 3): when computing a model explanation for a new query, it is safe to use previously released information, as it was computed in a differentially private manner. We use past information in two ways. Firstly, similar datapoints should have similar explanations: if \vec{z} and \vec{v} are very close to each other in the dataspace then the model explanations for \vec{v} and \vec{z} ($\phi^{Priv}(\vec{v})$ and $\phi^{Priv}(\vec{z})$) should be similar. This observation allows us to save time — and privacy budget — when computing new differentially private model explanations.

Secondly, instead of starting the gradient descent process in Algorithm 1 from an arbitrary point, we utilize past information to find an approximately optimal starting, resulting in faster convergence and reduced privacy spending. Ideally, we want to initialize the gradient descent process at a point as close to an optimal point as possible; however, this selection process should itself be privacy-preserving. Thus, the budget spent on finding the initialization point should not exceed the savings obtained by faster convergence.

Our explanation algorithm optimizes Equation 2, a convex function that has a unique minimum. This fact offers several indicators for a “good” starting point. Ideally, given the history $(\vec{z}_1, \phi^{Priv}(\vec{z}_1)), \dots, (\vec{z}_h, \phi^{Priv}(\vec{z}_h))$, we want to select $\phi^{Priv}(\vec{z}_j)$ minimizing $\|\phi^{Priv}(\vec{z}_j) - \phi^*(\vec{z}_{h+1})\|$. However, a tight bound on the sensitivity of $\min_j \|\phi^{Priv}(\vec{z}_j) - \phi^*(\vec{z}_{h+1})\|$ is difficult to obtain, as $\phi^*(z_{h+1})$ admits no closed-form solution; thus, searching for an initialization point results in a noisier selection process, requiring more undesirable privacy spending.

As an alternative, our adaptive differentially private algorithm uses a greedy approach: it searches for $\arg \min_j \|\nabla \mathcal{L}(\vec{z}_{h+1}, \phi^{Priv}(\vec{z}_j))\|$ which is a good indicator of one’s proximity to the optimum of the convex function $\mathcal{L}(\cdot)$. Moreover, the sensitivity of $\|\nabla \mathcal{L}(\vec{z}, \phi)\|$ is bounded by $\mathcal{O}(\frac{1}{m})$ (as per Lemma 3.1), which allows us to efficiently search for the optimal point while incurring minor privacy spending.

4.1 Finding Similar Points from Prior Explanation Queries

Consider the following weight function, defined for $c > 0$.

$$\alpha(\|\vec{x} - \vec{z}\|) = \begin{cases} 1, & \text{if } \|\vec{x} - \vec{z}\| \leq \frac{\sqrt{2c+1}-1}{2} \\ \frac{c}{2\|\vec{x}-\vec{z}\|(1+\|\vec{x}-\vec{z}\|)}, & \text{else} \end{cases} \quad (5)$$

This weight function α assigns equal weight to all points $\vec{x} \in \mathcal{X}$ that are close to the point of interest \vec{z} , and decreases the weight for points further from \vec{z} quadratically in their distance. This weight function (5) is bounded by 1, and belongs to $\mathcal{F}(c, \vec{z})$. Moreover, this weight function is “stable”: it preserves the consistency of the local explanation in a small region. We formalize this property in Lemma 4.1, and use the stable weight function in Equation (5) when running Algorithm 3.

In Lemma 4.1 we show that the stable weight function $\alpha(\cdot)$ evaluates two close queries \vec{v} and \vec{z} from the same region similarly. It shows that, if for two explanation queries \vec{v}, \vec{z} satisfy $\|\vec{v} - \vec{z}\| < d$, then the ratio of their weight functions is $1 + \mathcal{O}(d)$. This further shows that as d decreases, the stable weight function assigns similar weights to neighboring datapoints. This property is highly desirable when the underlying black-box model is consistent in local regions: it implies that the behavior of our explanation algorithm is also consistent in local regions. For the sake of exposition, we again write $r = \frac{\sqrt{2c+1}-1}{2}$, and assume that c (and in particular r) is a constant.

Lemma 4.1 (Stability of the $\alpha(\cdot)$ Function). *If $\|\vec{v} - \vec{z}\| \leq d$ then for all $\vec{x} \in \mathcal{X}$:*

$$\frac{\alpha(\|\vec{x} - \vec{v}\|)}{\alpha(\|\vec{x} - \vec{z}\|)} \leq 1 + \max\left(\frac{(d^2 + 2rd)}{r^2}, 2(d^2 + 2rd + d)\right).$$

Furthermore, if $d \in o(r)$ then $\frac{\alpha(\|\vec{x} - \vec{v}\|)}{\alpha(\|\vec{x} - \vec{z}\|)} < 1 + \mathcal{O}(d)$.

Proof. See Appendix C. □

Lemma 4.1 bounds the difference in α when $\|\vec{v} - \vec{z}\| \leq d \ll r$ for all $\vec{x} \in \mathcal{X}$. Theorem 4.2 shows that for the stable weight function, the queries \vec{v}, \vec{z} will have similar explanations if $\|\vec{v} - \vec{z}\| \leq d \leq r$. If $\phi^*(\vec{z})$ is the optimal solution of Equation 2 for \vec{z} , then Equation (10) shows that $\mathcal{L}(\phi^*(\vec{z}), \vec{v}, \mathcal{X}) \approx \mathcal{L}(\phi^*(\vec{z}), \vec{z}, \mathcal{X})$ when d is small.

Theorem 4.2. (Consistent Explanations in Small Regions) *For $\alpha(\cdot)$ described in (5), if we have $\phi^*(\vec{z}) \in \arg \min_{\phi \in \mathcal{C}} \mathcal{L}(\phi, \vec{z}, \mathcal{X})$, and $\phi^*(\vec{v}) = \arg \min_{\phi \in \mathcal{C}} \mathcal{L}(\phi, \vec{v}, \mathcal{X})$ and $\|\vec{x} - \vec{z}\| \leq d \ll r$, then*

$$\mathcal{L}(\phi^*(\vec{z}), \vec{v}, \mathcal{X}) - \mathcal{L}(\phi^*(\vec{v}), \vec{v}, \mathcal{X}) < 8d + \mathcal{O}(d^2).$$

Moreover, $|\mathcal{L}(\phi, \vec{v}, \mathcal{X}) - \mathcal{L}(\phi, \vec{z}, \mathcal{X})| \in \mathcal{O}(d^2)$ for all $\phi \in \mathcal{C}$

Proof. See Appendix D □

We use Theorem 4.2 to save our privacy budget when we receive two explanation queries from the same neighborhood. Suppose that the current queried point \vec{v} satisfies $\|\vec{v} - \vec{z}\| \leq d < r$, and \vec{z} is already explained in a differentially private manner. We can utilize the explanation for \vec{z} in order to compute an explanation for \vec{v} without spending any privacy budget with little approximation loss. However, this result only allows us to save the privacy budget if the query \vec{v} is in the region of some previously explained query \vec{z} .

4.2 Reusing Prior Explanations for a Better Optimization

Suppose that \vec{v} is not within a small region of \vec{z} , but the model exhibits similar behavior around \vec{z} and \vec{v} , i.e. $\|\nabla\mathcal{L}(\vec{\phi}^{Priv}(\vec{z}), \vec{v}, \mathcal{X})\|_2$ is sufficiently small; in this case, we can use the explanation of \vec{z} as an initialization point $\vec{\phi}^{\{0\}}$ for the gradient descent procedure used to generate an explanation for \vec{v} .

Theorem 4.4 shows that if $\|\nabla\mathcal{L}(\vec{\phi}^{Priv}(\vec{z}), \vec{v})\|_2$ is sufficiently small, then the gradient descent method initialized with $\phi^{\{0\}} = \phi^{Priv}(\vec{z})$ converges significantly faster when computing an explanation for \vec{v} . We also bound the number of iterations required in order to achieve same approximation error for our explanation compared to a random starting point, as a function of $\|\nabla\mathcal{L}(\phi^{\{0\}}, \vec{v}, \mathcal{X})\|$.

Before we prove the Theorem 4.4, we present a technical Lemma 4.3 in which we obtain the initialization dependent upper bound on the approximation error. Lemma 4.3 shows that the differentially private gradient descent algorithm converges faster when given a better initialization point, under minor assumptions. In particular, we show that for $T \leq e^{1/n\sigma^2}$, $\mathcal{E}(\phi^{\{T\}}, \vec{v}) = \frac{q \log T}{\sqrt{T}}$ where $q \leq 1$, and it decreases linearly in $\|\mathcal{L}(\phi^{\{0\}})\|$. Equation (11) provides the learning rate for the differentially private gradient descent algorithm. We note that in general the $\frac{q' \log T}{\sqrt{T}}$ bound holds for differentially private gradient descent when $\sqrt{n}\sigma \leq 1$ (see Theorem 3.2) where $q' > 1$ therefore $T \leq e^{1/n\sigma^2}$ is not an unreasonable assumption.

Recall that DPGD-Explain() in Algorithm 1 uses the following update rule:

$$\xi_t = \left(\phi^{\{t\}} - \eta(t) [\nabla\mathcal{L}(\phi, \mathcal{X}) + \mathcal{N}(0, \sigma^2\mathbf{I})] \right), \quad \phi^{\{t+1\}} = \arg \min_{\phi \in \mathcal{C}_{2,1}} \|\phi - \xi_t\| \quad (6)$$

Lemma 4.3 (Initialization Dependent Upper-Bound). *If $\|\nabla\mathcal{L}(\phi^{\{0\}}, \vec{v}, \mathcal{X})\| = \beta$, then for some c , and $\eta(t) = \frac{c}{\sqrt{t}}$;*

$$\mathcal{E}(\phi^{\{T\}}, \vec{x}) \in \mathcal{O} \left(\left((\sigma^2 n + \beta^2)^{\frac{1}{2}} + (n\sigma^2 \log T)^{\frac{1}{4}} \right) \frac{\log T}{\sqrt{T}} \right) \quad (7)$$

Proof. See Appendix E □

Theorem 4.4 (Number of Iterations). *Let $\phi^{\{0\}} = \phi^{Priv}(\vec{z})$ be the initialization point given to the DPGD-Explain() procedure, with $\|\nabla\mathcal{L}(\phi^{\{0\}}, \vec{v}, \mathcal{X})\| = \beta$. Given the update rule in Equation (6), if $\max(\sqrt{n}\sigma, \beta) \leq \frac{1}{(\log T)^a}$ for $a > \frac{1}{2}$, then for $T' = \max(\sqrt{n}\sigma, \beta)^{1-\frac{1}{2a}} T$: $\mathcal{E}(\phi^{\{T'\}}, \vec{v}) \in \mathcal{O} \left(\frac{\log T}{\sqrt{T}} \right)$.*

Proof. See Appendix F □

Our Adaptive approach uses Theorem 4.4 to reduce privacy spending, by accelerating the optimization process. If Algorithm 3 has already explained some query \vec{z} with a sufficiently small $\|\nabla\mathcal{L}(\phi^{Priv}(\vec{z}), \vec{v})\| = \beta$ then by initializing the optimization to $\phi^{\{0\}} = \phi^{Priv}(\vec{z})$, we require to spend some (β dependent) exponent of β factor of the total privacy required for the given approximation loss. Moreover, this exponent is a non-decreasing function of β , which ensures that better initialization points require fewer iterations to achieve a better approximation.

4.3 An Adaptive Explanation Protocol

The key idea of our algorithm is that once it releases enough information about the underlying explanation dataset, it utilizes this information to explain new queries with less privacy spending using Theorems 4.2 and 4.4.

Algorithm 2: Adaptive DP for Parameter Selection

Input: $\vec{z}_h \in \mathbb{R}^n$, explanation dataset \mathcal{X} , History \mathcal{H} , privacy spending for parameter selection ϵ_{para} , and the number of GD steps T , minimum variance σ_{min} ;

Output: Input variables for DPGD-Explain() for the query \vec{z}_h ;

```
1: Procedure Parameters-DPGD( $\vec{z}_h, \mathcal{H}, \epsilon_{para}, \sigma_{min}, \mathcal{X}, T$ )
2:   if  $\mathcal{H} == \emptyset$  then
3:     Arbitrary  $\phi \in \mathcal{C}_{2,1}$ ;
4:     return  $\phi, \sigma_{min}, T$ ;
5:   else
6:      $\phi^{best} \leftarrow \phi^{Priv}(\vec{z}_j)$  with  $\text{Pr} \propto \exp\left(-m \cdot \epsilon_{para} \cdot \frac{\|\nabla \mathcal{L}(\phi^{Priv}(\vec{z}_j), \vec{z}_h)\|}{2}\right)$  for  $\vec{z}_j \in \mathcal{H}$ 
7:      $\beta \leftarrow \|\nabla \mathcal{L}(\phi^{best}, \vec{z}_h)\|$ ;
8:      $\sigma \leftarrow \max\left(\frac{\beta}{\sqrt{n}}, \sigma_{min}\right)$ ;
9:      $a \leftarrow \frac{\log \frac{1}{\sqrt{n}\sigma}}{\log \log T}$ ; // Thm. 4.4
10:    if  $a > \frac{1}{2}$  then
11:       $T' \leftarrow (\sqrt{n}\sigma)^{1-\frac{1}{2a}} T$ ;
12:    else
13:       $T' \leftarrow T$ ;
14:    end
15:  end
16:  return  $\phi^{best}, \sigma, T'$ ;
```

Our mechanism (Algorithm 3) takes a total privacy budget (ϵ, δ) , a minimum privacy required for each query $(\epsilon_{min}, \delta_{min})$ (the maximum information leakage allowed per query), an explanation dataset \mathcal{X} , a maximal number of iterations T (which also defines the explanation quality requirement), and adaptively generates differentially private model explanations for a string of queries \vec{z}_1, \dots until it exhausts its entire privacy budget (ϵ, δ) .

Given the minimum privacy loss parameters $\epsilon_{min}, \delta_{min}$, we have a lower bound on the variance of Gaussian noise σ_{min} (Gaussian Mechanism [14]), added at each iteration, where ϵ_{ite} is computed using the composition theorem. This is the minimum variance required to achieve the resultant δ parameter with at least δ_{min} spent per query.

At each query \vec{z}_h , Algorithm 3 first inspects whether it has already explained some other data point \vec{z}_j using differentially private gradient decent algorithm such that $\|\vec{z}_h - \vec{z}_j\| < d$ in line 6. If such \vec{z}_j exists, it outputs $\phi^{Priv}(\vec{z}_j)$ for \vec{z}_h without any privacy spending, which is sufficiently accurate (Theorem 4.2). We note that if the explanation of \vec{z}_j was not computed from scratch (used explanation for some other $\vec{z}_{j'}, j' < j$) then we can not use the explanation of \vec{z}_j for \vec{z}_h because $\|\vec{z}_{j'} - \vec{z}_h\|$ might be $> d$. This is taken care by **Flag()** (see second condition of “if” statement in line 2 of Algorithm 3).

If there is no such \vec{z}_j , then our adaptive algorithm selects parameters for DPGD-Explain() adaptively exploiting past explained queries such that it converges faster with less privacy spending and lower approximation loss using Theorem 4.4. The adaptive parameter selection using history is explained in Algorithm 2. Given current explanation query, it picks $\phi^{Priv}(\vec{z}_j)$ with minimum $\|\nabla \mathcal{L}(\phi^{Priv}(\vec{z}_j), \vec{z}_h)\|$ as an initialization point for the gradient descent algorithm using a differentially private exponential mechanism [14]. It then computes the number of iterations required depending on the selected initialization point according to Theorem 4.4.

Algorithm 2 spends ϵ_{ite} differential privacy budget to choose the starting point. However,

Algorithm 3: Adaptive DP for Model Explanation

Input: Queries $\{\vec{z}_1, \dots\} \in \mathbb{R}^n$ arriving one by one, explanation dataset \mathcal{X} , privacy budget (ϵ, δ) , the minimum per-query privacy loss $(\epsilon_{min}, \delta_{min})$, and the number of GD steps T ;

```

1:  $\mathcal{H} \leftarrow \emptyset, \epsilon_{spent}, \delta_{spent} \leftarrow 0$ ;
2:  $\epsilon_{ite} \leftarrow \frac{\epsilon_{min}}{\sqrt{8T \log \frac{2}{\delta_{min}}}}$ ; // Privacy budget to spend per iteration
3:  $\sigma_{min} = \frac{\sqrt{2 \log(2.5T/\delta_{min})}}{m \cdot \epsilon_{ite}}$ ; // Variance needed for Gaussian mechanism
4:  $d \leftarrow \frac{\log T}{\sqrt{T}}$ ; // Distance bound required according to Thm. 4.2
5: for  $h = 1, \dots, \infty$  do
6:   if  $\exists \vec{z}_j \in \mathcal{H}$  with  $\|\vec{z}_h - \vec{z}_j\| \leq d$  &  $\text{Flag}(\vec{z}_j) = \top$  then
7:      $\phi^{Priv}(\vec{z}_h) \leftarrow \phi^{Priv}(\vec{z}_j)$ ; // Use a nearby point (Thm. 4.2)
8:     report:  $\phi^{Priv}(\vec{z}_h)$ ; // Report explanation of  $\vec{z}_h$ 
9:      $\mathcal{H}.append(\vec{z}_h : \phi^{Priv}(\vec{z}_h), \text{Flag}(\vec{z}_h) = \perp)$ 
10:  else
11:     $\phi^{best}, \sigma, T' \leftarrow \text{Parameters-DPGD}(\vec{z}_h, \mathcal{H}, \epsilon_{ite}, \sigma_{min}, \mathcal{X}, T)$ ;
12:     $\phi^{Priv}(\vec{z}_h) \leftarrow \text{DPGD-Explain}(\phi^{best}, \sigma, T')$ ;
13:    Update  $\epsilon_{spent}, \delta_{spent}$ ; // via the Strong Composition Theorem
14:    if  $\epsilon_{spent} > \epsilon$  or  $\delta_{spent} \geq \delta$  then
15:      | break; // Privacy budget is exhausted
16:    end
17:    report:  $\phi^{Priv}(\vec{z}_h)$ ;
18:     $\mathcal{H}.append(\vec{z}_h : \phi^{Priv}(\vec{z}_h), \text{Flag}(\vec{z}_h) = \top)$ ;
19:  end
20: end

```

even if $\|\nabla \mathcal{L}(\phi^{Priv}(\vec{z}_j), \vec{z}_h)\| \leq 1/\log T$ we need to run only $\sqrt{\beta}$ fraction of total iterations of the differentially private gradient descent algorithm and saves at least a $\beta^{\frac{1}{4}}$ factor of the privacy budget spent with lower approximation loss (Theorem 4.4).

Algorithm 3 is (ϵ, δ) - differentially private: all computation steps are conducted in a differentially private manner, and the total privacy budget spend does not exceed ϵ and δ .

Theorem 4.5 shows that Algorithm 3 achieves a nearly optimal approximation when $n \ll m$. Algorithm 3 is more efficient when the size of the explanation dataset m is much larger than the number of features n ; this decreases $\sqrt{n}\sigma_{min}$, allowing us to exploit smaller values of β . This trade-off between privacy saving and dimensionality is intuitive: in order to achieve a desirable level of privacy, differentially private gradient descent adds noise proportional to $\frac{\sqrt{n}}{m}$ at each iteration.

We can observe that the gain in approximation loss becomes negligible as t increases in comparison to the required extra privacy budget for that gain. More formally, the privacy budget for t iterations is $\mathcal{O}(\sqrt{t}\epsilon_{ite})$ by the Composition Theorem. This implies that the required privacy budget from iteration t to $t + 1$ is $\mathcal{O}(\epsilon_{ite}/\sqrt{t})$; on the other hand, the gain in approximation loss from iteration t to $t + 1$ is $\mathcal{O}(1/t^{\frac{3}{2}})$. Therefore we can stop after a small number of iterations. For example, for a dataset of size 10^8 , the optimal algorithm (in terms of approximation loss) suggests running 10^4 iterations, offering an approximation loss bounded by 0.19, whereas for 1000 iterations, the approximation loss is bounded by 0.22. The difference in privacy spending between the two instances is roughly $68\epsilon_{ite}$. Therefore, for practical purposes, one can use fewer iterations to save more privacy budget with only a negligent deprecation in approximation loss.

Theorem 4.5. (Utility Loss) Let $\phi^{Priv}(z_1), \dots, \phi^{Priv}(z_h)$ be the output of the Algorithm 3, then for all $j = 1, \dots, h$; $\mathcal{E}(\phi^{Priv}(z_j), \bar{z}_j) \in \mathcal{O}\left(\frac{\log T}{\sqrt{T}}\right)$. Moreover, for lower dimensional setting ($m > \frac{n}{\epsilon_{ite}}$) and $T = \sqrt{m}$: $\mathcal{E}(\phi^{Priv}(z_j), \bar{z}_j) \in \mathcal{O}\left(\log m/m^{\frac{1}{4}}\right)$

Proof. See Appendix G □

4.4 Early Termination and an Enhanced Adaptive Algorithm

Algorithm 3 is more efficient when the size of the explanation dataset m is much larger than the number of features n ; this decreases $\sqrt{n}\sigma_{min}$, allowing us to exploit smaller values of β . This trade-off between privacy saving and dimensionality is intuitive: in order to achieve a desirable level of privacy, differentially private gradient descent adds noise proportional to $\frac{\sqrt{n}}{m}$ at each iteration. Therefore, in high-dimensional settings, the noise required for privacy dominates the lower norm of the initial gradient and prevents Algorithm 3 from saving more of the privacy budget.

During the gradient descent optimization phase, if $\|\nabla\mathcal{L}(\phi^{\{t\}})\| \leq \sqrt{n}\sigma_{min}$, then Gaussian noise starts dominating $\nabla\mathcal{L}(\phi^{\{t\}})$. This domination by random Gaussian noise prevents further improvement in the loss function. Thus, the extra privacy budget spent once $\|\nabla\mathcal{L}(\phi^{\{t\}})\| \leq \sqrt{n}\sigma_{min}$ does not significantly improve explanation quality (approximation error); rather, it starts oscillating around the optimal point, resulting in slower convergence/decrease in approximation loss. Therefore, it is not beneficial to spend additional privacy budget once $\|\mathcal{L}(\phi^{\{t\}})\| < \sqrt{n}\sigma$; this observation is confirmed in Figure 4. This motivates us to define an unrestricted version of Algorithm 3, which maximizes possible savings by the initial point by iterating for $\max\{\beta^{1-\frac{1}{2a}}T, 2\}$ times for all queries, where a is the solution to $\beta = \frac{1}{\log^a T}$. The main intuition behind this approach is that whenever adaptive algorithm finds an initialization with $\beta = \|\mathcal{L}(\phi^{\{0\}})\| \ll \sqrt{n}\sigma_{min}$ then increasing the number of iterations does not result in faster convergence as Gaussian noise dominates: privacy spending in these cases offers little improvement in loss.

To implement the enhanced adaptive algorithm, we only change Line 8 to $T' \leftarrow \beta^{1-1/2a}T$ (instead of $\sqrt{n}\sigma^{1-1/2a}T$) in Algorithm 2 where $a = \frac{\log 1/\beta}{\log \log T}$. We do not maintain a similar general theoretical bound on the approximation error as in Algorithm 3; however, we empirically analyze the performance of the enhanced adaptive algorithm in Section 6 (see Figures 2 and 3 for privacy spending and approximation loss).

4.5 Last Phase: Non-Interactive DP Mechanisms for Model Explanation

While Algorithm 3 spends less privacy budget than Algorithm 1, it will eventually exhaust its privacy budget after explaining finitely many datapoints. However, by explaining a sufficiently large number of datapoints, we gather enough information to generate explanations for new queries, *without spending any additional privacy budget*.

Let \mathcal{H} be the history of the explanation queries and their explanation generated by Algorithm 3 using a total privacy budget of (ϵ, δ) . We propose a *non-interactive phase* algorithm for generating model explanations, which takes \mathcal{H} the output of Algorithm 3 as input, and generates an explanation for new queries without spending any *additional* privacy budget. The main idea of this approach is that if \mathcal{H} contains enough information about the underlying black-box model that, making additional queries to the explanation dataset \mathcal{X} unnecessary. We can rather use the explanations already given to the user (adversary) and their own dataset to explain additional queries.

Algorithm 4: Non-Interactive DP for Model Explanation

Input: Privately explained history \mathcal{H} where $h = |\mathcal{H}|$, List of point of interest queries $\{\vec{z}_h, \dots\} \in \mathbb{R}^n$ arriving one by one;

- 1: $\mathcal{X}' = \{\vec{z}_1, \dots, \vec{z}_h\}, \hat{f}(\cdot)$; // According to section 4.5
- 2: **for** $i = h+1, \dots$ **do**
- 3: $\phi^{Priv}(\vec{z}_i) = \arg \min_{\phi \in \mathcal{C}_{2,1}} \mathcal{L}(\phi, \vec{z}_h, \mathcal{X}', \hat{f}(\cdot))$;
- 4: **report:** $\phi^{Priv}(\vec{z}_i)$; // Report explanation of \vec{z}_i
- 5: **end**

We construct a *proxy explanation dataset* using the history \mathcal{H} which contains explained datapoints and their corresponding differentially private explanation. The proxy explanation dataset is simply $\mathcal{X}' = \{\vec{z}_1, \dots, \vec{z}_h : \vec{z}_j \in \mathcal{H}\}$, i.e. the points queried by the user. Their labels are the corresponding model explanations, which are linear approximations of the original model: $\hat{f}(\mathcal{X}') = \{\phi^{Priv}(\vec{z}_j)^\top \cdot \vec{z}_j : j = 1, \dots, h\}$. Given a new query \vec{z} , we generate a new query via a linear approximation of the black box model around \vec{z} using \mathcal{X}' and the corresponding differentially private approximation $\hat{f}(\mathcal{X}')$.

$$\phi^{Priv}(\vec{z}, \mathcal{H}) = \arg \min_{\phi \in \mathcal{C}} \sum_{\vec{z}_j \in \mathcal{X}'} \alpha(\|\vec{z}_j - \vec{z}\|) (\phi^\top \cdot (\vec{z}_j - \vec{z}) - \hat{f}(\vec{z}_j))^2 \quad (8)$$

The non-interactive phase is described in Algorithm 4 with details. It takes \mathcal{H} history as an input which consists of differentially private explanations of past queries and computes explanations for further explanation queries. The non-interactive phase generates an explanation for a new query \vec{z} by optimizing (8) which provides a linear approximation of the black-box model around the point \vec{z} . However, we do not need to spend any privacy budget for generating a private explanation for \vec{z} as it does not use the explanation dataset \mathcal{X} for any further computations and $\hat{f}(\cdot)$ is already computed using differential privacy [14]. This allows the adaptive version to explain infinitely many queries even after the entire privacy budget has been spent. We evaluate the performance of the non-interactive phase in Section 6.

5 Protecting the Privacy of the Training Dataset

The analysis in Sections 3 and 4 shows that our mechanisms protect the *explanation dataset*. In what follows, we analyze their *training data* (\mathcal{T}) privacy guarantees.

The only potential source of training data information leakage is the gradients computed by our algorithm at each iteration. Our algorithms inject Gaussian noise to the gradient of the loss function at each iteration; fortunately, this noise injection offers some privacy guarantees with respect to the training dataset. We quantify the improvement in the privacy guarantees of the training dataset due to the randomness inserted by our explanation algorithms when the underlying training process is $(\hat{\epsilon}, \hat{\delta})$ -differentially private. By the post-processing property of the differential privacy [14], explanations generated by our algorithm are already $(\hat{\epsilon}, \hat{\delta})$ -differentially private, however, in Theorem 5.1, we show that our explanations improve the privacy guarantees for the training dataset. We also show that even if the training process is non-differentially private (training process doesn't provide any protection for the training dataset), our explanation algorithms provide $(\mathcal{O}(m\epsilon), \delta)$ -differential privacy.

Theorem 5.1 (Privacy amplification for the training dataset). *Suppose that the underlying training process of the black-box model f is $(\hat{\epsilon}, \hat{\delta})$ -differentially private w.r.t. the training dataset, then the explanation algorithm described in Algorithm 1 with parameters (ϵ, δ) is $(\hat{\epsilon}, \gamma\hat{\delta})$ -differentially private for the training dataset, where, $\gamma \in 1 - \mathcal{O}\left(\left(\frac{\log \frac{T}{\delta}}{m\epsilon}\right) \left(e^{-\frac{m\epsilon}{\log(\frac{T}{\delta})}}\right)\right)$. Moreover for any training process, Algorithm 1 is $(\mathcal{O}(m\epsilon), \delta)$ -differentially private for the training dataset.*

Proof. See Appendix H □

Theorem 5.1 (proven in Appendix H) shows that our privacy guarantees with respect to the training set grow weaker as the size of the explanation dataset (the parameter m) increases; this presents a natural tradeoff between the amount of data used by the mechanisms generating model explanations, and the privacy guarantees we can offer with respect to the training data.

At first glance, our guarantees seem rather weak - growing linearly worse in m . However, our bound is tight: consider the (extremely unstable) training where the label of all datapoints in the dataspace depends on the presence of a single data record in the training dataset; if this point is present then all labels are +1, and are -1 otherwise. Protecting against information leaks in this example is nearly impossible, irrespective of the model explanation mechanism [29, 30].

6 Experimental Results

We evaluate our model explanations on standard machine learning datasets. We use the following benchmark datasets (we use the datasets in their entirety as the explanation dataset \mathcal{X}):

ACS13: We use a scrubbed version of the dataset used in [10]¹ containing 1,494,974 records and predict income ($> 50k\$$ vs $\leq 50k\$$). We train a random forest classifier with 500 trees with maximum depth = 10, which achieves 85% training accuracy and 84% test accuracy.

IMDB/Amazon Movie Reviews (Text dataset) [22, 26]: This dataset consists of 8,765,568 movie reviews from the Amazon review dataset along with 50,000 movie reviews from IMDB large review dataset mapped to binary vector using the top 500 words. Each movie review is labeled as either a positive (+1) or a negative (-1) review. We consider the true labels as the output of some unknown black-box algorithm.

Facial expression dataset [16] This dataset consists of 12,156 48×48 pixel grayscale images of faces. We train a CNN with two convolution layers with 5×5 filters followed by max-pooling and a fully connected layer, achieving training and test accuracy of 86% and 84.3%, respectively. We use this dataset to demonstrate the visualization of our explanations.

We repeat experiments 10 times, and plot their average behavior.

6.1 Interactive DP Model Explanation

We use our non-adaptive protocol (Algorithm 1) to generate private model explanations for points in all datasets. We compare the explanations we generate with existing non-private model agnostic explanation methods. In the Text dataset, we generate differentially private model explanations for 1000 randomly sampled datapoints (movie reviews) from the dataset with strong privacy parameters $\epsilon = 0.1$ and $\delta = 10^{-6}$. We present a few examples in Table 2. The explanations generated by our protocol agree with well-established non-private model agnostic explanations: using LIME [27] and MIM [33], we extract the top 5 most influential words. According to our

¹Pulled from <http://www.census.gov/programs-surveys/acs/>.

Table 2: Examples of influence measures generated for Text movie reviews dataset by Algorithm 1 with $\epsilon \approx 0.1$ and $\delta = 10^{-6}$, LIME and MIM. Upwards (downwards) arrows indicate a high positive (negative) influence of a word. Moreover blue, red and green arrows correspond to words selected to Algorithm 1, LIME, and MIM.

	Movie Review	label
1.	... year Batman ... attempted make well ↑↑ acted De Vito ... bad ↓↓↓ intentions ... searching past would ↓↓ like ... given bad ↓↓↓ reviews...	+1
2.	... superb ↑↑↑ performance by Natalie Portman... saying script bad ↓ at times but I don't ↓↓↓...The film look ↑ bad, don't good ↑ direction and excellent ↑↑ performances ↑↑...	+1
3.	Yeah adults may find stupid ↑↑↑... don't ↑↑ think really bad.... The story ↓ aAlvin gang... across world search jewels bad ↑↑↑ with... So animation good ↓ ...	-1
4.	I never seen such horrible ↑↑ special affects or acting... I laughed ↓↓↓ so hard on this its just stupid ↑ I mean the movie is so awful ↑↑↑...	-1

Table 3: Summary of mean \pm Variance of loss in utility for each dataset for explanation generated by Algorithm 1 (Theorem 3.2).

Dataset	$\epsilon = 0.01, \delta = 10^{-6}$	$\epsilon = 0.1, \delta = 10^{-6}$
Face	$1.4 \times 10^{-2} \pm 4.3 \times 10^{-3}$	$2.2 \times 10^{-3} \pm 2.1 \times 10^{-4}$
Text	$2.7 \times 10^{-3} \pm 7.8 \times 10^{-4}$	$4.3 \times 10^{-4} \pm 9.4 \times 10^{-6}$
ACS13	$5.7 \times 10^{-3} \pm 1.3 \times 10^{-3}$	$2.6 \times 10^{-4} \pm 6.3 \times 10^{-5}$

evaluation, our protocol and MIM share 2.6 of the top 5 influential words on average, whereas our protocol and LIME share 3.9 words on average, with a variance of less than 0.3 in both cases.

How does explanation quality degrade as we make our privacy requirements more stringent? This can be visually observed for the facial expression dataset by generating explanation by Algorithm 1 with different ϵ values, and a fixed $\delta = 10^{-5}$ (Figure 1); Algorithm 1 generates explanations that appear meaningful with $\epsilon \geq 0.07$ and $\delta = 10^{-5}$.

We compare the loss of our explanation algorithm defined in Equation (4) for different privacy parameters ϵ on 1000 randomly selected datapoints from the datasets. We compute the mean \pm variance value of the approximation loss for ACS13 and Text dataset for $\epsilon = 0.01$ and $\epsilon = 0.1$ with $\delta = 10^{-6}$ (Table 3). The loss decreases as we relax privacy requirements (this follows from Theorem 3.2). We compute better explanations for the Text dataset than the ACS13 dataset; this can be explained by their different dimensionality (the \sqrt{n}/m factor in Theorem 3.2).

6.2 Saving the Privacy Budget via the Adaptive Approach

We analyze both privacy spending and loss in our adaptive protocols, as compared to the baseline non-adaptive protocol (Algorithm 1). We randomly sample three batches of 1500 datapoints and divide the explanation dataset into three equal-sized, disjoint parts.

We run parallel composition [23] for our private explanations by separately using the three

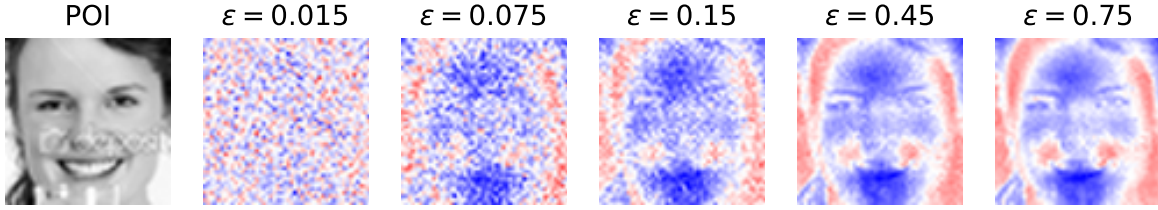
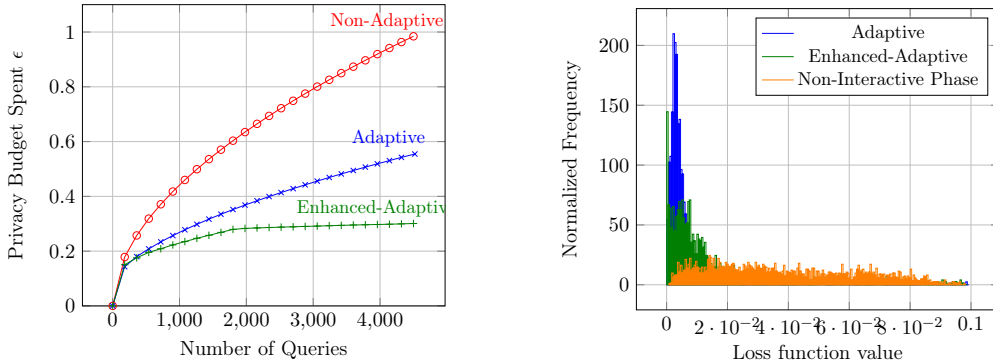
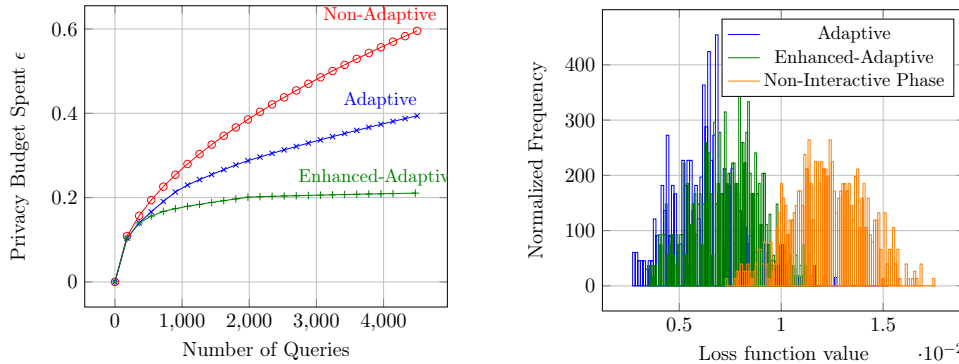


Figure 1: The effect of varying ϵ on explanation quality of Algorithm 1. The color blue (red) indicates positive (negative) influence. Brighter colors indicate greater influence.



(a) Total privacy budget spent by the non-adaptive (Algorithm 1), adaptive (Algorithm 3) and enhanced adaptive algorithms on the same sample for the ACS13 dataset. (b) Normalized loss histogram for queries explained by the adaptive, enhanced adaptive and non-interactive mechanisms for the ACS13 dataset. Adaptive approaches exhibit lower loss, trading off privacy and utility.

Figure 2: Explanation quality and privacy guarantees for the ACS13 dataset.



(a) Total privacy budget spent by the non-adaptive (Algorithm 1), adaptive (Algorithm 3) and enhanced adaptive algorithms on the same sample for the Text dataset. (b) Normalized loss histogram for queries explained by the adaptive, enhanced adaptive and non-interactive mechanisms for the Text dataset. Adaptive approaches exhibit lower loss, trading off privacy and utility.

Figure 3: Sub-figure 3a shows the total privacy budget spent by the non-adaptive (Algorithm 1), adaptive (Algorithm 3) and enhanced adaptive algorithms on the same sample for the Text dataset. The x -axis represents the number of queries answered, and the y -axis shows the value of privacy parameter ϵ . Sub-figure 3b is the normalized loss histogram for queries explained by the adaptive, enhanced adaptive and Non-interactive phase. The adaptive approach has a lower loss than the non-interactive phase, a natural trade-off between privacy and utility.

disjoint explanation datasets to explain three sequences of 1500 queries. We predefine a desired level of loss guarantee; in other words, both model explanations must achieve the same explanation quality, to ensure a valid comparison. We set the per-query ϵ parameter to $\epsilon = 0.01$ for the ACS13 dataset, and to $\epsilon = 0.006$ for the Text dataset. In both evaluations we set $\delta = 10^{-7}$, and set the maximal number of DPGD-Explain() iterations to $T = 300$. This upper bound is only reached for 94/4500 (73/4500) queries for the Text(ACS13) dataset. In all other cases, the adaptive algorithms were able to find a better initialization point. See Figure 5 for more details.

Interestingly, for the Text (ACS13) data, on average, over 1850 (2220) instances had a better initialization point, which failed to satisfy the $\sqrt{n}\sigma_{min} \leq \beta$ condition, and thus had to proceed with $T' = 91$ ($T' = 95$) (the minimum iterations theoretically required according to Theorem 4.4. We note that this minimum T' improves as we relax our privacy requirements (Theorem 4.4), allowing the adaptive algorithm to save more of the privacy budget. The improved performance for the ACS13 dataset may be explained by the fact that it consists of dense regions, as compared to the Text dataset.

We analyze privacy spending and loss values (Equation 1) by different algorithms in Figure 2 (ACS13) and Figure 3 (Text). The adaptive protocols spend most of their privacy budget on the initial ~ 100 queries; after they generate enough information, they capitalize on it to explain the remaining queries using a smaller per-query privacy budget. Furthermore, the adaptive protocols achieve the same explanation quality as the non-adaptive protocol, while utilizing a much smaller privacy budget (as predicted by Theorem 4.5). Figures 2b and 3b show that the Adaptive and Enhanced-Adaptive protocols exhibit a similar distribution of loss values, with a significant difference in the privacy spending rate. This can be explained by the dominance of Gaussian noise over the “good” initialization point.

In Figure 4, we plot the convergence of DPGD-Explain for 15 randomly selected data points for which Algorithm 3 found an initialization point with $\beta < \sqrt{n}\sigma_{min}$ (line 8 of Algorithm 2). We observe that after the first few iterations, Gaussian noise dominates and increases the loss value; only later does it converge to a loss close to the initial point in such cases. This results in extra spending of privacy without any gain in approximation loss. This empirically explains the similar distribution of explanation quality by adaptive and enhanced adaptive algorithms (Figures 2b and 3b) despite that enhanced adaptive algorithm iterates less number of iterations compare to adaptive algorithm and spends significant lesser privacy budget (Figures 2b and 3b).

Once Algorithm 3 explains 4500 queries, we use its output to generate additional explanations in the Non-Interactive Phase (without spending any further privacy budget) for another randomly sampled 4500 datapoints for both datasets. The non-interactive phase exhibits higher loss, but spends none of the privacy budget (Figure 3).

6.3 Differentially Private Explanation for Differentially Private Models

We train differentially private neural networks (all with the same architecture) on the IMDB Dataset [22] using the Tensorflow differential privacy library [4]; we obtain differentially private models of the form $f_{\hat{\epsilon}}$ with different privacy parameters $\hat{\epsilon} = 0.5, 2, 10$ and $\hat{\delta} = 10^{-5}$. The models are trained on the same training and test dataset, split in a 70 : 30 ratio (35,000 training reviews and 15,000 test reviews). The models $f_{0.5}, f_2, f_{10}$ achieve a test accuracy of 52%, 74%, 81% respectively. We also train a non-private model, f , which achieves a test accuracy of 83.6%.

We also train differentially private neural networks (all with the same architecture) on the Face Dataset, with privacy parameters $\hat{\epsilon} = 0.5, 2, 10$ and $\hat{\delta} = 10^{-5}$. They achieve a test accuracy of 51%, 62% and 80% respectively. We also train a non-private model, f , which achieves test

Loss value over iterations for Algorithm 3

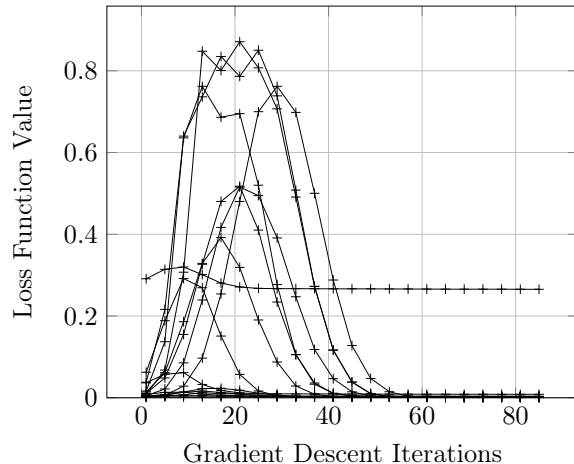


Figure 4: The convergence pattern of DP gradient descent for 15 randomly selected from explained queries for ACS13 dataset by Algorithm 3, where $\sigma_{min} > \frac{\beta}{\sqrt{n}}$ for the initial point, line 8 of Algorithm 2. This is where the initial point is close to the optimal point. The noise variance pushes the *good* initialization away from the optimal point, only to re-converge to nearly the same level.

accuracy of 84.3%. The models are trained on the same training and test dataset split into 70 : 30 ratio (number of training images = 8510 and test images = 3646).

We generate private explanations (Algorithm 1 with $\epsilon = 0.1, \delta = 10^{-5}$ and $T = 200$) for all models for the same randomly sampled 500 datapoints. We compare the private explanation for the POI for the different private models with the base optimal explanation for the non-private model. We compute the distortion (**Dist**) for each POI and DP models: $\text{Dist}(\vec{x}, f_{\hat{\epsilon}}) = \|\phi^{Priv}(\vec{x}, f_{\hat{\epsilon}}) - \phi^*(\vec{x}, f)\|$. **Dist** captures the change in the models’ behavior around POI due to noise added in the training process. We plot the histogram of the **Dist** values in Figure 7(a) observe that the **Dist** values are much larger for the model $f_{0.5}$, compared to f_{10} . This is intuitive: for smaller $\hat{\epsilon}$, model becomes noisier and uses random features for the classification. We further analyze this visually.

In Figure 6, we visually represent the explanation generated for different private models for an image which was misclassified as a happy face by all models. When the privacy requirements are extremely high ($\hat{\epsilon} = 0.5$), feature influence is randomly distributed: this informally shows that the modal randomly classified the image as a happy face; however, as we relax the privacy requirements of the training dataset, the model explanation becomes more constructive, utilizing important features. For example, pixels around lips start having high positive influence.

We plot the histogram of the approximation error (Equation 4) in Figure 7(b) and observe that the approximation error is higher for the model $f_{0.5}$. As $f_{0.5}$ becomes noisy, it assigns labels randomly around POI. This unpredictable behavior of the model around POI requires more iterations to converge to the optimal linear approximation. Indeed, differentially private models with strong privacy guarantees are difficult to approximate by the `DPGD-Explain()` procedure spending more of the privacy budget for the same level of approximation loss.

To evaluate the impact of noisy/random model behavior around the POI, and the explanation approximation error, we plot the approximation error vs misclassification error of the model around a POI in Figure 8. For all differentially private models, there is a positive correlation

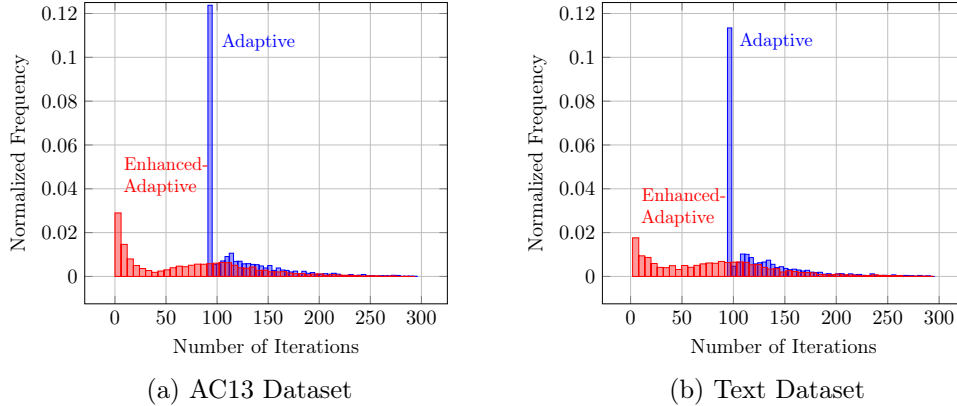


Figure 5: The normalized histogram of the number of DP gradient descent iterations by the Adaptive Algorithm (Algorithm 3) and the Enhanced-Adaptive algorithm for the ACS13 and Text datasets. This spike for the Adaptive algorithm is due to minimum required iterations. For both the ACS13 and Text dataset, the Enhanced-Adaptive approach iterates less than 90 times per query in most instances. The notable spike at around 100 iterations is due to several samples running the theoretically required number of iterations for Algorithm 3 to provably maintain its quality guarantees. See Theorem 4.4 and Line 8 of Algorithm 2 for the related theoretical analysis. Overall, Algorithm 3 ran 149 iterations on average for the Text dataset, and 121 for the ACS13 dataset. The Enhanced-Adaptive algorithm runs for 28 iterations and 43 iterations on average, respectively.

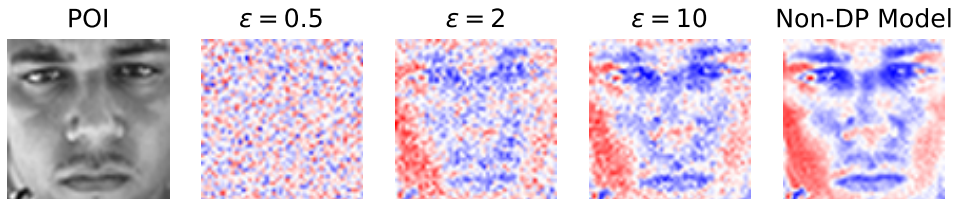


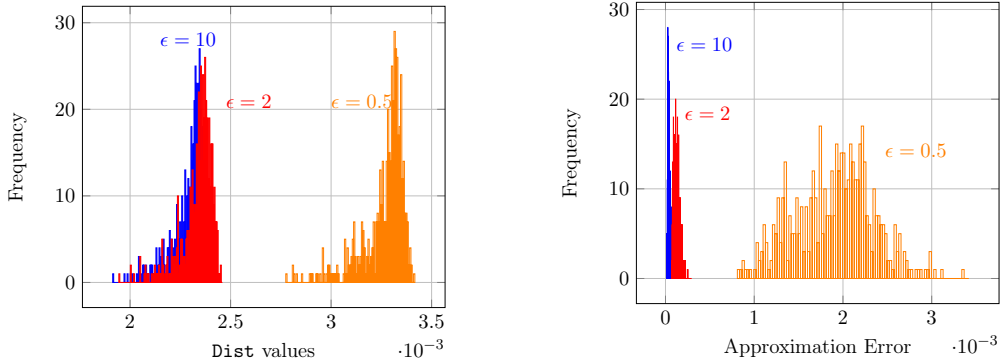
Figure 6: The effect of differential private models on the explanation. The color blue (red) indicates positive (negative) influence. Brighter colors indicate greater influence.

between explanation approximation and model misclassification error. For all models and POIs, we use the same input parameters to generate private explanations ($\epsilon = 0.1, \delta = 10^{-5}, T = 500$). This empirically confirms that when the model “misbehaves”, randomly assigning labels around the POI, private explanations exhibit a higher approximation error. This further shows that differentially private models with strong privacy guarantees require more privacy budget for the explanation dataset to achieve a similar level of explanation quality. This also explains the higher approximation loss for $f_{0.5}$ compared to f_2, f_{10} observed in Figure 7(b).

6.4 The Effect of Data Density

The effectiveness of Algorithm 3 relies, in part, on the existence of points with low gradient loss (denoted by β); such points are often close to the query point. To evaluate this effect, we compare the performance of Algorithm 3 in densely and sparsely sampled queries.

We first cluster the dataset using a hierarchical clustering algorithm. We observe that while



(a) The `Dist` values for different models over the same sampled datapoints. (b) Explanation approximation loss for different models over the same sampled datapoints.

Figure 7: Histograms of `Dist` values and explanation quality for different DP models. The approximation error and explanation quality for the model $f_{0.5}$ is higher compared to f_2, f_{10} , likely due to the complicated decision boundaries around POI for noisier models.

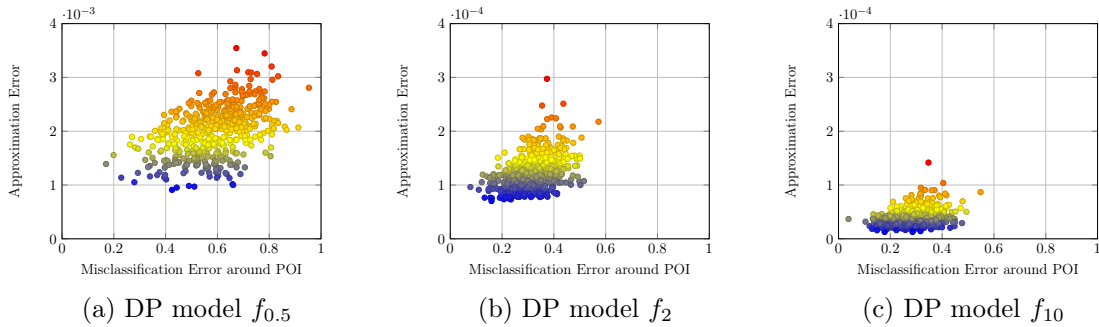


Figure 8: The approximation vs misclassification error around the POI (50 nearest points to the POI) for all DP models. The explanation quality deprecates as the model becomes more inconsistent around the POI with a positive correlation for all models (note the different y axis max for Figures 8b and 8c). Privacy requirements result in noisier models, which results in additional privacy spending for our explanations algorithms.

the Text dataset is well-distributed and sparse in the dataspace, the ACS13 dataset has over 15 different clusters with different population densities. We sample in three different regimes: first, we randomly sample three samples of size 800 from the dataset (this serves as our baseline); second, we randomly sample three samples of 800 datapoints from the densest cluster; finally, we sample datapoints from different clusters to intentionally sparsify the sample. We then query each set of sampled points with Algorithm 3 in parallel composition with $\epsilon_{min} = 10^{-2}$ and $T = 300$.

Indeed, as shown in Figure 9a, sparse samples lead to greater expenditure of the privacy budget than dense samples. A likely explanation for this phenomenon is that densely sampled queries exhibit consistent behavior from the black-box classifier, allowing more efficient exploitation of past information by Algorithm 3. That said, it may be the case that two disparate regions in the dataspace exhibit similar classifier behavior; in this scenario, Algorithm 3 can exploit previously computed explanations from different regions.

6.5 The Effects of Overfitting

Intuitively, overfitted models yield more complex decision boundaries, to achieve better training accuracy. According to our hypotheses, Algorithm 3 needs to spend more privacy budget to explain the overfitted models compare to the non-overfitted model. We train an overfitted random decision forest with 500 trees with maximum depth = 60 on ACS13 dataset which achieves 98% training accuracy and 80% test accuracy. We first identify the overfitted data regions: we find clusters of training data that exhibit a significant difference in training accuracy between the overfitted and non-overfitted models.

We randomly sample three samples of 500 data points from the overfitted region, and run Algorithm 3 on these samples in parallel with $T = 300$ and $\epsilon_{min} = 10^{-2}$ for both over-fitted and non-over-fitted models. Figure 9b indicates that Algorithm 3 requires a higher privacy budget to explain the overfitted model as compared to the non-overfitted model.

Moreover, Algorithm 3 needs to compute an average of 87 queries from the sample with full computation whereas, for a non-overfitted model, 58 queries required full computation on average. After an initial ≈ 150 queries on average, Algorithm 2 fails to satisfy the $\sqrt{n}\sigma_{min} \leq \beta$ (line 8 of Algorithm 2) condition for both overfitted and non-overfitted models and proceeds with $T' = 95$ for most instances in all cases.

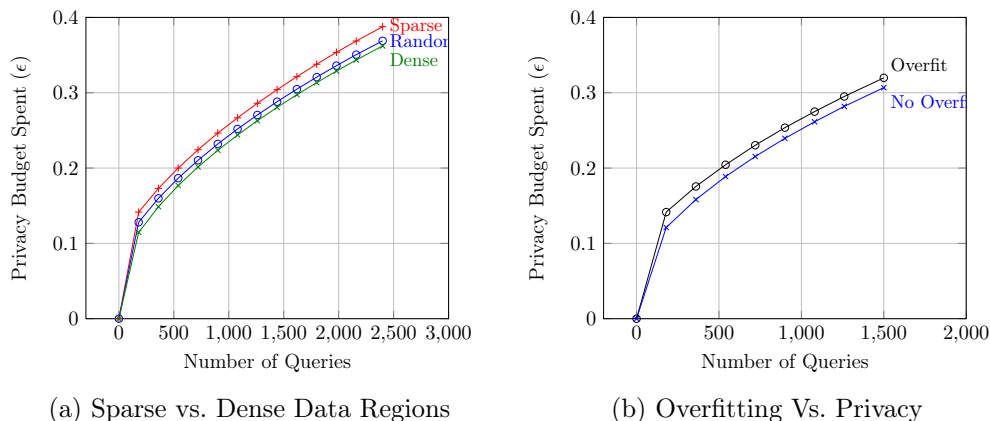


Figure 9: Figure 9a shows the privacy budget spent by Algorithm 3 on sparse/dense/random samples from the ACS13 dataset. Figure 9b demonstrates the privacy budget spent by Algorithm 3 on an overfitted/non-overfitted model on the ACS13 dataset. The x -axis shows the number of queries answered; the y -axis is the privacy budget spent - ϵ .

7 Broader Impact

Transparency in AI has become an important research topic; however, as recent works show, model transparency poses potential risks to user privacy. Our approach provably protects against adversaries trying to recover data used in generating explanations. Several data companies are now offering model explanations as part of their ML suites²: if unsafe model explanations are offered in high stakes domains (say, in explaining users' financial or medical data as we do in our work), they offer a novel avenue for attack that has been relatively unexplored. Our methodology

²e.g. IBM <http://aix360.mybluemix.net/>, Microsoft <https://docs.microsoft.com/en-us/azure/machine-learning/how-to-machine-learning-interpretability> and Google's <https://cloud.google.com/explainable-ai> frameworks.

is easy to implement, and offers provable privacy and quality guarantees; thus, if our protocols are implemented in such services, users are guaranteed to receive good explanations that protect their personal data; the authors see this as a *positive* impact on society.

Our methodology does carry some risks. Our results uniformly support the existence of a tradeoff between user privacy and explanation quality. This tradeoff can be seen both through our theoretical results and empirical analysis, and applies to both the privacy of the explanation dataset and the model training data. This tradeoff seems to be particularly sharp in regions where the model overfits, and for high-dimensional data. The actual effects of this tradeoff are highly implementation and data dependent, and require further analysis as to the exact risks they hold. It could very well be that there exist alternative modes of model explanation that offer more favorable privacy/quality tradeoffs (or indeed, no tradeoffs whatsoever); the authors believe that this is not the case. We believe that there is a general theory of model explanations and user privacy: useful model explanations leak some information, and that leakage needs to be managed from a privacy perspective. Applying our techniques does require some care: one immediate concern is *disparate impact*. Regions where the model overfits to the data tend to suffer more from privacy/quality tradeoffs; in other words, when implementing our system on real high-stakes systems, it is important to ensure that minority groups are not adversely affected in unacceptable ways. It is undesirable to offer low-quality model explanations to minorities, but it is also undesirable to risk leaking their private information. This tradeoff has been alluded to in [29], and is formally proven in our work. While it is entirely possible that this tradeoff only exists due to the shortcomings of this work, we strongly suspect that it is a universal truth: model explanations inevitably leak private information, and must undergo some degradation — noise induced or otherwise — before being released. This risk must certainly be assessed carefully in any future implementation of our work.

8 Conclusions

In this work, we provide a formal framework for studying differential privacy in model explanations. Not only are our model explanation methods differentially private, they are also approximately optimal. Our methods are *safe and sound*: offering both quality and privacy guarantees. There are still many interesting open problems regarding the design of model explanations that simultaneously protect both the training and explanation datasets from exposure, while retaining explanation accuracy.

While our work focuses on the interplay between privacy and transparency, it follows some recent insights on the effects of privacy mechanisms on model accuracy. As we demonstrate in Sections 6.4 and 6.5, sparse data regions and overfitted models lead to poorer performance, either in terms of explanation accuracy, or in terms of required privacy budget. Such data regions often correspond to underrepresented population groups; our results echo those in recent works [7, 29]: indeed, differential privacy injects more noise to model explanations offered to minority groups. Assessing the privacy/explainability tradeoffs for minority groups is a promising avenue for future exploration.

Acknowledgments

This work was supported by the National Research Foundation Singapore, AI Singapore award number AISG-RP-2018-009, grant number R-252-000-A20-490.

References

- [1] Philip Adler, Casey Falk, Sorelle A Friedler, Tionney Nix, Gabriel Rybeck, Carlos Scheidegger, Brandon Smith, and Suresh Venkatasubramanian. Auditing black-box models for indirect influence. *Knowledge and Information Systems*, 54(1):95–122, 2018.
- [2] Marco Ancona, Enea Ceolini, Cengiz Öztireli, and Markus Gross. A unified view of gradient-based attribution methods for deep neural networks. In *Proceedings of the NIPS 2017 Workshop on Interpreting, Explaining and Visualizing Deep Learning*, 2017.
- [3] Marco Ancona, Enea Ceolini, Cengiz Öztireli, and Markus Gross. Towards better understanding of gradient-based attribution methods for deep neural networks. In *Proceedings of the 6th International Conference on Learning Representations (ICLR)*, pages 1–16, 2018.
- [4] Galen Andrew, Steve Chien, and Nicholas Papernot. Tensorflow privacy library, 2019. <https://github.com/tensorflow/privacy>.
- [5] Sebastian Bach, Alexander Binder, Grégoire Montavon, Frederick Klauschen, Klaus-Robert Müller, and Wojciech Samek. On pixel-wise explanations for non-linear classifier decisions by layer-wise relevance propagation. *PLoS one*, 10(7):e0130140, 2015.
- [6] David Baehrens, Timon Schroeter, Stefan Harmeling, Motoaki Kawanabe, Katja Hansen, and Klaus-Robert Müller. How to explain individual classification decisions. *Journal of Machine Learning Research*, 11(Jun):1803–1831, 2010.
- [7] Eugene Bagdasaryan, Omid Poursaeed, and Vitaly Shmatikov. Differential privacy has disparate impact on model accuracy. In *Proceedings of the 32nd Annual Conference on Neural Information Processing Systems (NeurIPS)*, pages 15453–15462, 2019.
- [8] Borja Balle, Gilles Barthe, Marco Gaboardi, and Joseph Geumlek. Privacy amplification by mixing and diffusion mechanisms. In *Proceedings of the 32nd Annual Conference on Neural Information Processing Systems (NeurIPS)*, pages 13277–13287, 2019.
- [9] S. S. Barsov and Vladimir V. Ulyanov. Estimates of the proximity of Gaussian measures. In *Soviet Mathematics Doklady*, volume 34, pages 462–466, 1987.
- [10] Vincent Bindschaedler, Reza Shokri, and Carl A Gunter. Plausible deniability for privacy-preserving data synthesis. *Proceedings of the VLDB Endowment*, 10(5):481–492, 2017.
- [11] Amit Datta, Anupam Datta, Ariel D Procaccia, and Yair Zick. Influence in classification via cooperative game theory. In *Proceedings of the 24th International Joint Conference on Artificial Intelligence (IJCAI)*, pages 511–517, 2015.
- [12] Anupam Datta, Matthew Fredrikson, Gihyuk Ko, Piotr Mardziel, and Shayak Sen. Use privacy in data-driven systems: Theory and experiments with machine learnt programs. In *Proceedings of the 24th ACM SIGSAC Conference on Computer and Communications Security (CCS)*, pages 1193–1210, 2017.
- [13] Anupam Datta, Shayak Sen, and Yair Zick. Algorithmic transparency via quantitative input influence: Theory and experiments with learning systems. In *Proceedings of the 37th IEEE Symposium on Security and Privacy (Oakland)*, pages 598–617. IEEE, 2016.

- [14] Cynthia Dwork. Differential privacy. In *Proceedings of the 33rd International Colloquium on Automata, Languages and Programming (ICALP)*, pages 1–12, 2006.
- [15] Cynthia Dwork and Aaron Roth. The algorithmic foundations of differential privacy. *Foundations and Trends in Theoretical Computer Science*, 9(3–4):211–407, 2014.
- [16] Ian J Goodfellow, Dumitru Erhan, Pierre Luc Carrier, Aaron Courville, Mehdi Mirza, Ben Hamner, Will Cukierski, Yichuan Tang, David Thaler, Dong-Hyun Lee, et al. Challenges in representation learning: A report on three machine learning contests. *Neural Networks*, 64:59–63, 2015.
- [17] Riccardo Guidotti, Anna Monreale, Salvatore Ruggieri, Franco Turini, Fosca Giannotti, and Dino Pedreschi. A survey of methods for explaining black box models. *ACM Computing Surveys*, 51(5):93:1–93:42, August 2018.
- [18] Frederik Harder, Matthias Bauer, and Mijung Park. Interpretable and differentially private predictions. In *Proceedings of the 34th AAAI Conference on Artificial Intelligence (AAAI)*, pages 4083–4090, 2020.
- [19] Peter Kairouz, Sewoong Oh, and Pramod Viswanath. The composition theorem for differential privacy. *IEEE Transactions on Information Theory*, 63(6):4037–4049, 2017.
- [20] Zachary Chase Lipton. The mythos of model interpretability. *CoRR*, abs/1606.03490, 2016.
- [21] Scott M Lundberg and Su-In Lee. A unified approach to interpreting model predictions. In *Proceedings of the 31st Annual Conference on Neural Information Processing Systems (NIPS)*, pages 4765–4774, 2017.
- [22] Andrew L Maas, Raymond E Daly, Peter T Pham, Dan Huang, Andrew Y Ng, and Christopher Potts. Learning word vectors for sentiment analysis. In *Proceedings of the 49th Annual Meeting of the Association for Computational Linguistics: Human Language Technologies (HLT)*, pages 142–150, 2011.
- [23] Frank D McSherry. Privacy integrated queries: an extensible platform for privacy-preserving data analysis. In *Proceedings of the 2009 ACM Conference on Management of Data (SIGMOD)*, pages 19–30, 2009.
- [24] Smitha Milli, Ludwig Schmidt, Anca D. Dragan, and Moritz Hardt. Model reconstruction from model explanations. In *Proceedings of the 2nd Conference on Fairness, Accountability, and Transparency (FAT*)*, pages 1–9, 2019.
- [25] Milad Nasr, Reza Shokri, and Amir Houmansadr. Comprehensive privacy analysis of deep learning: Passive and active white-box inference attacks against centralized and federated learning. In *Proceedings of the 40th IEEE Symposium on Security and Privacy (Oakland)*, pages 739–753, 2019.
- [26] Jianmo Ni, Jiacheng Li, and Julian McAuley. Justifying recommendations using distantly-labeled reviews and fine-grained aspects. In *Proceedings of the 15th Conference on Empirical Methods on Natural Language Processing (EMNLP)*, pages 188–197, 2019.

- [27] Marco Tulio Ribeiro, Sameer Singh, and Carlos Guestrin. Why should i trust you?: Explaining the predictions of any classifier. In *Proceedings of the 22nd International Conference on Knowledge Discovery and Data Mining (KDD)*, pages 1135–1144, 2016.
- [28] Ohad Shamir and Tong Zhang. Stochastic gradient descent for non-smooth optimization: Convergence results and optimal averaging schemes. In *Proceedings of the 30th International Conference on Machine Learning (ICML)*, pages 71–79, 2013.
- [29] Reza Shokri, Martin Strobel, and Yair Zick. Privacy risks of explaining machine learning models. *CoRR*, abs/1907.00164, 2019.
- [30] Reza Shokri, Marco Stronati, Congzheng Song, and Vitaly Shmatikov. Membership inference attacks against machine learning models. In *Proceedings of the 38th IEEE Symposium on Security and Privacy (Oakland)*, pages 3–18, 2017.
- [31] Avanti Shrikumar, Peyton Greenside, and Anshul Kundaje. Learning important features through propagating activation differences. In *Proceedings of the 34th International Conference on Machine Learning (ICML)*, pages 3145–3153, 2017.
- [32] Karen Simonyan, Andrea Vedaldi, and Andrew Zisserman. Deep inside convolutional networks: Visualising image classification models and saliency maps. *arXiv preprint arXiv:1312.6034*, 2013.
- [33] Jakub Sliwinski, Martin Strobel, and Yair Zick. A characterization of monotone influence measures for data classification. In *Proceedings of the 33rd AAAI Conference on Artificial Intelligence (AAAI)*, pages 718–725, 2019.
- [34] Daniel Smilkov, Nikhil Thorat, Been Kim, Fernanda B. Viégas, and Martin Wattenberg. Smoothgrad: removing noise by adding noise. *CoRR*, abs/1706.03825, 2017.
- [35] Mukund Sundararajan, Ankur Taly, and Qiqi Yan. Axiomatic attribution for deep networks. In *Proceedings of the 34th International Conference on Machine Learning (ICML)*, pages 3319–3328, 2017.

A Proof of Lemma 3.1

Lemma 3.1 (Conditions for Bounded Sensitivity for $\nabla L(\cdot)$). *For all explanation dataset \mathcal{X} of size m , and all its neighboring datasets \mathcal{X}' , points of interest \vec{z} , and $\phi \in \mathcal{C}$, the sensitivity of the gradient of loss is bounded, $\|\nabla \mathcal{L}(\phi, \mathcal{X}) - \nabla \mathcal{L}(\phi, \mathcal{X}')\|_2 \leq (\frac{c}{m})$, iff $\alpha(\|\vec{x} - \vec{z}'\|) \leq \frac{c}{2\|\vec{x} - \vec{z}'\|_2(\|\vec{x} - \vec{z}'\|_2 + 1)}$ for every $\vec{x}, \vec{z}' \in \mathbb{R}^n$.*

Proof. We first note that

$$\nabla \mathcal{L}(\phi, \mathcal{X}) = \frac{2}{m} \sum_{\vec{x} \in \mathcal{X}} \alpha(\|\vec{x} - \vec{x}'\|) (\phi^\top (\vec{x} - \vec{x}') - f(\vec{x})) (\vec{x} - \vec{x}')$$

Now, for $\alpha(\|\vec{x} - \vec{x}'\|) \leq \frac{c}{2\|\vec{x} - \vec{x}'\|_2(\|\vec{x} - \vec{x}'\|_2 + 1)}$ and any $\vec{x}' \in \mathcal{X}$, $\|\nabla \mathcal{L}(\phi, \mathcal{X}) - \nabla \mathcal{L}(\phi, \mathcal{X} \setminus \{\vec{x}'\})\|_2$

$$\begin{aligned} &\leq \frac{2}{m} \alpha(\|\vec{x}' - \vec{x}\|) ((\phi^\top (\vec{x} - \vec{x}') - f(\vec{x})) (\vec{x} - \vec{x}')) \\ &\leq \frac{2}{m} \alpha(\|\vec{x}' - \vec{x}\|) (\|\phi\|_2 \|\vec{x} - \vec{x}'\|_2 - f(\vec{x})) \leq \frac{c}{m} \end{aligned}$$

all inequalities are tight, which concludes the proof. \square

B Proof of Theorem 3.2

Theorem 3.2 (Bounded Utility Loss). *Algorithm 1 is (ϵ, δ) differentially private. Moreover, for given privacy parameters (ϵ, δ) , if DPGD-Explain() runs for $T \leq \min\left(\frac{m^2 \epsilon^2}{32n \log^2(e+1/\delta)}, \frac{1}{\delta}\right)$ iterations and outputs an explanation ϕ^{Priv} , then $\mathcal{E}(\phi^{Priv}) \in \mathcal{O}\left(\frac{\log T}{\sqrt{T}}\right)$. For $T = \frac{m^2 \epsilon^2}{32n \log^2(e+1/\delta)}$, $\mathcal{E}(\phi^{Priv}) \in \mathcal{O}\left(\frac{\sqrt{n \log m}}{m\epsilon}\right)$.*

Proof. Theorem 2 in [28] shows that for a gradient descent algorithm $\phi_{t+1} \leftarrow \Gamma_{\mathcal{C}}(\phi_t - \eta(t)\hat{g}(t))$ with $\mathbb{E}[\hat{g}(t)] = \nabla \mathcal{L}(\phi, \mathcal{X})$, $\eta(t) = \frac{c}{\sqrt{t}}$ and $\mathbb{E}(\|\hat{g}(t)\|^2) \leq G^2$,

$$\mathbb{E}[\mathcal{L}(\phi^{Priv}, \mathcal{X}, c)] - \min_{\phi \in \mathcal{C}} \mathcal{L}(\phi, \mathcal{X}, c) \leq \left(\frac{1}{c} + cG^2\right) \frac{2 + \log T}{\sqrt{T}}$$

The above bound minimize for $c = \frac{1}{G}$. By putting $C = \frac{1}{G}$, we get

$$\mathbb{E}[\mathcal{L}(\phi^{Priv}, \mathcal{X}, c)] - \min_{\phi \in \mathcal{C}} \mathcal{L}(\phi, \mathcal{X}, c) \leq 2G \times \frac{2 + \log T}{\sqrt{T}}$$

In Algorithm 1, $\hat{g}(t) = \nabla \mathcal{L}(\phi, \mathcal{X}) + \vec{Z}$, where $Z_i \sim \mathcal{N}(0, \sigma^2 \mathbf{I})$. As $\mathbb{E}(\vec{Z}) = \vec{0}$, we can write $\mathbb{E}(\|\hat{g}(t)\|^2)$ as

$$\begin{aligned} \mathbb{E}(\|\hat{g}(t)\|^2) &= \|\nabla \mathcal{L}(\phi, \mathcal{X})\|^2 + \mathbb{E}\left[\sum_{i=1}^n Z_i^2\right] \\ &\leq 1 + \frac{16Tn \log(e + \sqrt{T}\epsilon/\delta) \log \frac{T}{\delta}}{m^2 \epsilon^2} \end{aligned}$$

For $T \leq \frac{m^2 \epsilon^2}{32n \log^2(e+\epsilon/\delta)}$, $G \leq \sqrt{2}$ which implies that $\mathcal{E}(\phi^{Priv}) \in \log\left(\frac{\log T}{\sqrt{T}}\right)$

Also for $T > \frac{m^2 \epsilon^2}{32n \log^2(e+\epsilon/\delta)}$; function $2G \times \frac{2+\log T}{\sqrt{T}}$ increases as T increases. Therefore by setting $T = \frac{m^2 \epsilon^2}{32n \log^2(e+\epsilon/\delta)}$ for the optimal upper bound, we get

$$\mathcal{E}(\phi^{Priv}) \in \mathcal{O}\left(\frac{\sqrt{n} \log\left(\frac{1}{\delta}\right) \log(m\epsilon/\sqrt{n})}{m\epsilon}\right)$$

For large m , ignoring the $\log \frac{1}{\delta}$ term,

$$\mathcal{E}(\phi^{Priv}) \in \mathcal{O}\left(\frac{\sqrt{n} \log(m/\sqrt{n})}{m\epsilon}\right)$$

□

C Proof of Lemma 4.1

Lemma 4.1 (Stability of the $\alpha(\cdot)$ Function). *If $\|\vec{v} - \vec{z}\| \leq d$ then for all $\vec{x} \in \mathcal{X}$:*

$$\frac{\alpha(\|\vec{x} - \vec{v}\|)}{\alpha(\|\vec{x} - \vec{z}\|)} \leq 1 + \max\left(\frac{(d^2 + 2rd)}{r^2}, 2(d^2 + 2rd + d)\right).$$

Furthermore, if $d \in o(r)$ then $\frac{\alpha(\|\vec{x} - \vec{v}\|)}{\alpha(\|\vec{x} - \vec{z}\|)} < 1 + \mathcal{O}(d)$.

Proof. We first note that when $\|\vec{x} - \vec{z}\| \leq r$ $\frac{\alpha(\|\vec{x} - \vec{v}\|)}{\alpha(\|\vec{x} - \vec{z}\|)} = \frac{\alpha(\|\vec{x} - \vec{v}\|)}{1} \leq 1$ since $\alpha(\cdot) \leq 1$ on any input. Thus, we analyse the case when $\|\vec{v} - \vec{z}\| > r$. If $\|\vec{x} - \vec{v}\| \leq r$ then:

$$\begin{aligned} \frac{\alpha(\|\vec{x} - \vec{v}\|)}{\alpha(\|\vec{x} - \vec{z}\|)} &= \frac{1}{\frac{c}{2\|\vec{x} - \vec{z}\|(1 + \|\vec{x} - \vec{z}\|)}} \\ &= \frac{2\|\vec{x} - \vec{z}\|(1 + \|\vec{x} - \vec{z}\|)}{c} \leq \frac{2(r+d)(1+r+d)}{c} \\ &= \frac{2(r^2 + r) + 2(d^2 + 2rd)}{c} = 1 + \frac{2(d^2 + 2rd)}{c} \end{aligned}$$

Now, for $\|\vec{x} - \vec{v}\| > r$: if $\|\vec{x} - \vec{v}\| \geq \|\vec{x} - \vec{z}\|$ then by definition of the weight function, $\frac{\alpha(\|\vec{x} - \vec{v}\|)}{\alpha(\|\vec{x} - \vec{z}\|)} \leq 1$. Therefore we analyse the case when $\|\vec{x} - \vec{v}\| < \|\vec{x} - \vec{z}\|$;

$$\frac{\alpha(\|\vec{x} - \vec{v}\|)}{\alpha(\|\vec{x} - \vec{z}\|)} = \frac{(\|\vec{x} - \vec{z}\|)(1 + \|\vec{x} - \vec{z}\|)}{(\|\vec{x} - \vec{v}\|)(1 + \|\vec{x} - \vec{v}\|)}$$

As we know, $\|\vec{x} - \vec{z}\| \leq d$; $\|\vec{x} - \vec{z}\| \leq d + \|\vec{x} - \vec{v}\|$. By using this inequality;

$$\begin{aligned} \frac{\alpha(\|\vec{x} - \vec{v}\|)}{\alpha(\|\vec{x} - \vec{v}\|)} &\leq \frac{(d + \|\vec{x} - \vec{v}\|)(1 + \|\vec{x} - \vec{v}\| + d)}{(\|\vec{x} - \vec{v}\|)(1 + \|\vec{x} - \vec{v}\|)} \\ &\leq \left(1 + \frac{d}{r}\right) \left(1 + \frac{d}{r+1}\right) \leq 1 + \frac{d^2 + 2rd}{r^2} \end{aligned}$$

Which shows that for all $\vec{x} \in \mathcal{X}$

$$\frac{\alpha(\|\vec{x} - \vec{v}\|)}{\alpha(\|\vec{x} - \vec{z}\|)} \leq 1 + \max\left(\frac{(d^2 + 2rd)}{r^2}, \frac{2(d^2 + 2rd + d)}{c}\right)$$

Finally, suppose that $d \in o(r)$; in this case, $\frac{(d^2+2rd)}{r^2} < d \times \frac{3}{r} \in \mathcal{O}(d)$, and

$$\frac{2(d^2 + 2rd + d)}{c} < \frac{d(3r + 1)}{c} \in \mathcal{O}(d),$$

which shows that, for $d \in o(r)$

$$\frac{\alpha(\|\vec{x} - \vec{v}\|)}{\alpha(\|\vec{x} - \vec{z}\|)} \leq 1 + \mathcal{O}(d) \quad , \forall \vec{x} \in \mathcal{X} \quad (9)$$

□

D Proof of Theorem 4.2

Next, let us prove Theorem 4.2.

Theorem 4.2. (Consistent Explanations in Small Regions) *For $\alpha(\cdot)$ described in (5), if we have $\phi^*(\vec{z}) \in \arg \min_{\phi \in \mathcal{C}} \mathcal{L}(\phi, \vec{z}, \mathcal{X})$, and $\phi^*(\vec{v}) = \arg \min_{\phi \in \mathcal{C}} \mathcal{L}(\phi, \vec{v}, \mathcal{X})$ and $\|\vec{x} - \vec{z}\| \leq d \ll r$, then*

$$\mathcal{L}(\phi^*(\vec{z}), \vec{v}, \mathcal{X}) - \mathcal{L}(\phi^*(\vec{v}), \vec{v}, \mathcal{X}) < 8d + \mathcal{O}(d^2).$$

Moreover, $|\mathcal{L}(\phi, \vec{v}, \mathcal{X}) - \mathcal{L}(\phi, \vec{z}, \mathcal{X})| \in \mathcal{O}(d^2)$ for all $\phi \in \mathcal{C}$

Proof. First, $\mathcal{L}(\phi^*(\vec{z}), \vec{v}, \mathcal{X})$ equals:

$$\begin{aligned} & \frac{1}{m} \sum_{\vec{x} \in \mathcal{X}} \alpha(\|\vec{x} - \vec{v}\|) (\phi^*(\vec{z})^\top (\vec{x} - \vec{v}) - f(\vec{x}))^2 = \\ & \frac{1}{m} \sum_{\vec{x} \in \mathcal{X}} \alpha(\|\vec{x} - \vec{v}\|) (\phi^*(\vec{z})^\top (\vec{x} - \vec{z}) - f(\vec{x}) + \phi^*(\vec{z})^\top (\vec{z} - \vec{v}))^2 \\ & \leq \frac{1}{m} \sum_{\vec{x} \in \mathcal{X}} \alpha(\|\vec{x} - \vec{v}\|) (\phi^*(\vec{z})^\top (\vec{v} - \vec{z}) - f(\vec{x}))^2 + d^2 \\ & \quad + \frac{d}{m} \sum_{y \in \mathcal{X}} \alpha(\|\vec{x} - \vec{v}\|) |\phi^*(\vec{z})^\top (\vec{x} - \vec{z}) - f(\vec{x})| \end{aligned}$$

Now, for $\|\vec{v} - \vec{z}\| \leq d < r$;

$$\alpha(\|\vec{x} - \vec{v}\|) |\phi^*(\vec{z})^\top (\vec{x} - \vec{z}) - f(\vec{x})| \leq (1 + d + r)$$

and $\alpha(\|\vec{x} - \vec{v}\|) \leq 1$. By Lemma 4.1, $\alpha(\|\vec{x} - \vec{v}\|) \leq (1 + \mathcal{O}(d))\alpha(\|\vec{x} - \vec{z}\|)$, which implies that $\mathcal{L}(\phi^*(\vec{z}), \vec{v}, \mathcal{X})$ is upper bounded by

$$\begin{aligned} & \frac{1 + \mathcal{O}(d)}{m} \sum_{\vec{x} \in \mathcal{X}} \alpha(\|\vec{x} - \vec{z}\|) (\phi^*(\vec{z})^\top (\vec{x} - \vec{z}) - f(\vec{x}))^2 + (2 + r)d + \mathcal{O}(d^2) \leq \\ & \frac{1 + \mathcal{O}(d)}{m} \sum_{\vec{x} \in \mathcal{X}} \alpha(\|\vec{x} - \vec{z}\|) (\phi^*(\vec{v})^\top (\vec{x} - \vec{v}) - f(\vec{x}) \phi^*(\vec{v})^\top (\vec{v} - \vec{z}))^2 + (2 + r)d + \mathcal{O}(d^2) \end{aligned}$$

Invoking Lemma 4.1 again we have $\alpha(\|\vec{x} - \vec{z}\|) \leq (1 + \mathcal{O}(d))\alpha(\|\vec{x} - \vec{v}\|)$, and the last inequality follows from the fact that $\mathcal{L}(\phi^*(\vec{z}), \vec{z}, \mathcal{X}) \leq \mathcal{L}(\phi^*(\vec{v}), \vec{z}, \mathcal{X})$. By combining these results, $\mathcal{L}(\phi^*(\vec{z}), \vec{v}, \mathcal{X})$ is upper bounded by

$$\leq (1 + \mathcal{O}(d))^2 \mathcal{L}(\phi^*(\vec{v}), \vec{v}, \mathcal{X}) + 2(2 + r)d + \mathcal{O}(d^2)$$

Now, $\mathcal{L}(\phi^*(\vec{v}), \vec{v}, \mathcal{X}) \leq \mathcal{L}(\vec{0}, \vec{v}, \mathcal{X}) \leq 1$, Which shows that,

$$\mathcal{L}(\phi^*(\vec{z}), \vec{v}, \mathcal{X}) - \mathcal{L}(\phi^*(\vec{v}), \vec{v}, \mathcal{X}) \leq (6 + 2r)d + \mathcal{O}(d^2) \quad (10)$$

and concludes the proof of the first part. For the second part, take any $\phi \in \mathcal{C}$, then $|\mathcal{L}(\phi, \vec{v}, \mathcal{X}) - \mathcal{L}(\phi, \vec{z}, \mathcal{X})|$

$$\leq \frac{\mathcal{O}(d^2)}{m} \sum_{\vec{x} \in \mathcal{X}} \alpha(\|\vec{x} - \vec{v}\|)(\|\vec{x} - \vec{v}\| + \|\vec{x} - \vec{z}\| + 2)$$

Now, if $\|\vec{x} - \vec{v}\| \leq r$ then $\alpha(\|\vec{x} - \vec{v}\|)(\|\vec{x} - \vec{v}\| + \|\vec{x} - \vec{z}\| + 2) \leq (2(r + 2) + d)$ and if $\|\vec{x} - \vec{v}\| > r$ then $\alpha(\|\vec{x} - \vec{v}\|)(\|\vec{x} - \vec{v}\| + \|\vec{x} - \vec{z}\| + 2) \leq (1 + \frac{r+d+1}{r})$, which shows that, for all $\phi \in \mathcal{C}$;

$$|\mathcal{L}(\phi, \vec{v}, \mathcal{X}) - \mathcal{L}(\phi, \vec{z}, \mathcal{X})| \in \mathcal{O}(d^2)$$

□

E Proof of Lemma 4.3

Lemma 4.3 (Initialization Dependent Upper-Bound). *If $\|\nabla \mathcal{L}(\phi^{\{0\}}, \vec{v}, \mathcal{X})\| = \beta$, then for some c , and $\eta(t) = \frac{c}{\sqrt{t}}$;*

$$\mathcal{E}(\phi^{\{T\}}, \vec{x}) \in \mathcal{O}\left(\left((\sigma^2 n + \beta^2)^{\frac{1}{2}} + (n\sigma^2 \log T)^{\frac{1}{4}}\right) \frac{\log T}{\sqrt{T}}\right) \quad (7)$$

Proof. The proof of the lemma uses [28, Theorem 2]. We denote $g_t = \eta(t)[\nabla \mathcal{L}(\phi^{\{t\}}, \vec{v}, \mathcal{X}) + \mathcal{N}(0, \sigma^2 \mathbf{I})]$ and $\mathcal{L}(\phi^{\{t\}}, \vec{v}, \mathcal{X})$ by $\mathcal{L}(\phi^{\{t\}})$. By extending the inequality in [28, Equation (2)] we obtain;

$$\mathbb{E}[g_t^\top (\phi^{\{t\}} - \phi^{\{T-k\}})] \leq \frac{1}{2c}[\sqrt{T} - \sqrt{T-k}] + \frac{1}{2} \sum_{t=T-k}^T \frac{c\mathbb{E}[\|g_t\|^2]}{\sqrt{t}}$$

Now, we know that $\|\nabla \mathcal{L}(\phi^{\{0\}})\|^2 = \beta^2$. By using Taylor's Theorem we get,

$$\begin{aligned} \nabla \mathcal{L}(\phi^{\{t+1\}}) &= \nabla \mathcal{L}(\phi^{\{t\}}) + \nabla^2 \mathcal{L}(\phi^{\{t\}})(\phi^{\{t+1\}} - \phi^{\{t\}}) \\ &= (\mathbf{I} - \eta(t)\nabla^2 \mathcal{L}(\phi^{\{t\}}))\nabla \mathcal{L}(\phi^{\{t\}}) - \eta(t)\nabla^2 \mathcal{L}(\phi^{\{t\}})Z_t \end{aligned}$$

Where $Z_t \sim \mathcal{N}(0, \sigma^2 \mathbf{I})$. As $\nabla^2 \mathcal{L}(\phi^{\{t\}})$ is a semi-positive-definite matrix with $\|\nabla^2 \mathcal{L}(\phi^{\{t\}})\| \leq 1$,

$$\begin{aligned} \mathbb{E}[\|\nabla \mathcal{L}(\phi^{\{t+1\}})\|^2] &\leq \mathbb{E}[\|\nabla \mathcal{L}(\phi^{\{t\}})\|^2] + \eta^2(t)n\sigma^2 \leq \\ &\mathbb{E}[\|\nabla \mathcal{L}(\phi_0)\|^2] + n\sigma^2 \sum_{l=1}^t \frac{c^2}{l} \leq \beta^2 + n\sigma^2 c^2 \log t \\ &\leq \beta^2 + n\sigma^2 c^2 \log T \end{aligned}$$

Therefore $\mathbb{E}[\|g_t\|^2] \leq (\beta^2 + n\sigma^2) + n\sigma^2 c^2 \log T$. As $\mathcal{L}(\cdot)$ is a convex function, by [28, Theorem 2], we obtain,

$$\mathcal{E}(\phi^{\{T\}}, \vec{x}) \leq \left(\frac{1}{c} + c(n\sigma^2 + \beta^2) + c^3 n\sigma^2 \log T \right) \frac{(\log T + 2)}{\sqrt{T}}$$

The above bound is minimized for the positive solution of: $-\frac{1}{c^2} + (n\sigma^2 + \beta^2) + 3n\sigma^2 c^2 = 0$. Which implies that the above bound minimizes for,

$$c^2 = \frac{2}{\left((n\sigma^2 + \beta^2) + \sqrt{(n\sigma^2 + \beta^2)^2 + 12n\sigma^2 \log T} \right)} \quad (11)$$

Plugging back the optimal c , we get

$$\mathcal{E}(\phi^{\{T\}}, \vec{x}) \in \mathcal{O} \left(\left((\sigma^2 n + \beta^2)^{\frac{1}{2}} + (n\sigma^2 \log T)^{\frac{1}{4}} \right) \frac{\log T}{\sqrt{T}} \right)$$

Which concludes the proof. \square

F Proof of Theorem 4.4

Let us now prove Theorem 4.4.

Theorem 4.4 (Number of Iterations). *Let $\phi^{\{0\}} = \phi^{Priv}(\vec{z})$ be the initialization point given to the DPGD-Explain() procedure, with $\|\nabla \mathcal{L}(\phi^{\{0\}}, \vec{v}, \mathcal{X})\| = \beta$. Given the update rule in Equation (6), if $\max(\sqrt{n}\sigma, \beta) \leq \frac{1}{(\log T)^a}$ for $a > \frac{1}{2}$, then for $T' = \max(\sqrt{n}\sigma, \beta)^{1-\frac{1}{2a}} T$: $\mathcal{E}(\phi^{\{T\}}, \vec{v}) \in \mathcal{O} \left(\frac{\log T}{\sqrt{T}} \right)$.*

Proof. Let $b = \max(\sqrt{n}\sigma, \beta)$, substituting $T' = bT$ into Lemma 4.3, we get,

$$\mathcal{E}(\phi^{\{T\}}, \vec{v}) \in \mathcal{O} \left(\frac{b^{\frac{1}{2}} \log^{\frac{5}{4}}(bT)}{b^{\frac{1}{2} - \frac{1}{4a}} T^{\frac{1}{2}}} \right)$$

For $b \leq \frac{1}{(\log T)^a}$, $b^{\frac{1}{4a}} \log^{\frac{5}{4}}(bT) \leq \log T$, which implies that $\mathcal{E}(\phi^{\{T\}}, \vec{v}) \in \mathcal{O} \left(\frac{\log T}{T^{\frac{1}{2}}} \right)$, concluding the proof. \square

G Proof of Theorem 4.5

Theorem 4.5. (Utility Loss) *Let $\phi^{Priv}(z_1), \dots, \phi^{Priv}(z_h)$ be the output of the Algorithm 3, then for all $j = 1, \dots, h$; $\mathcal{E}(\phi^{Priv}(z_j), \vec{z}_j) \in \mathcal{O} \left(\frac{\log T}{\sqrt{T}} \right)$. Moreover, for lower dimensional setting ($m > \frac{n}{\epsilon_{ite}}$) and $T = \sqrt{m}$: $\mathcal{E}(\phi^{Priv}(z_j), \vec{z}_j) \in \mathcal{O} \left(\log m / m^{\frac{1}{4}} \right)$*

Proof. Theorem 4.5 is a corollary of Theorem 4.2, Theorem 4.4 and Theorem 3.2. First, if the **If** condition in *line 2* of Algorithm 3 is satisfied, then as $l < k$, by Theorem 4.2,

$$\begin{aligned} & |\mathcal{L}(\phi^{Priv}(\vec{z}_j), \vec{z}_j) - \mathcal{L}(\phi^*(\vec{z}_j), \vec{z}_j)| \leq |\mathcal{L}(\phi^{Priv}(\vec{z}_j), \vec{z}_j) \\ & - \mathcal{L}(\phi^{Priv}(\vec{z}_j), \vec{x})| + |\mathcal{L}(\phi^{Priv}(\vec{z}_j), \vec{x}) - \mathcal{L}(\phi^*(\vec{z}_j), \vec{z}_j)| \\ & \in \mathcal{O}(\log^2 T / T) + \mathcal{O}(\log T / \sqrt{T}) \in \mathcal{O} \left(\frac{\log T}{\sqrt{T}} \right) \end{aligned}$$

For other cases; by Theorem 3.2 and Theorem 4.4;

$$\mathcal{E}(\phi^{Priv}(\vec{z}_j), \vec{z}_j) \in \mathcal{O}\left(\frac{\log T}{\sqrt{T}}\right)$$

By substituting $T = \sqrt{m}$, we get that $\mathcal{E}(\phi^{Priv}(z_j), \vec{z}_j) \in \mathcal{O}\left(\log m/m^{\frac{1}{4}}\right)$, which concludes the proof. \square

H Proof of Theorem 5.1

Before we prove Theorem 5.1, we prove the following technical lemma.

Lemma H.1. *If X, Y and Z are random variables defined on the same probability space with same compact range \mathcal{R} and $X \perp Z$, $Y \perp Z$ and $X \perp Y$ then the total variation distance,*

$$\text{TV}(X + Z, Y + Z) \leq \max_{x,y} \text{TV}(X + Z|X = x, Y + Z|Y = y)$$

Proof. The definition of the Total variation distance between two distribution is defined as

$$\begin{aligned} \text{TV}(X + Z, Y + Z) &= \sup_E (\Pr[X + Z \in E] - \Pr[Y + Z \in E]) \\ &= \sup_E \left(\int_{\mathcal{R}} \Pr[x + Z \in E] f_X(x) dx - \int_{\mathcal{R}} \Pr[y + Z \in E] f_Y(y) dy \right) \\ &\leq \sup_E \left(\max_x \Pr[x + Z \in E] \int_{\mathcal{R}} f_X(x) dx - \min_y \Pr[y + Z \in E] \int_{\mathcal{R}} f_Y(y) dy \right) \\ &= \sup_E \left(\max_x \Pr[x + Z \in E] - \min_y \Pr[y + Z \in E] \right) \end{aligned} \quad (12)$$

Where f_X and f_Y denotes the density function of the probability distribution of X and Y . Now if $X = x^*$ and $Y = y^*$ maximize the difference $\max_{x,y} (\Pr[Z + x \in E] - \Pr[Z + y \in E])$ for any E , that implies that $x^* = \arg \max \Pr[Z + x \in E]$ and $y^* = \arg \min \Pr[Z + y \in E]$. The equality in Equation 12 follows from the fact that f_X and f_Y are probability densities. This shows that

$$\begin{aligned} \text{TV}(X + Z, Y + Z) &\leq \sup_E \left(\max_{x,y} (\Pr[x + Z \in E] - \Pr[y + Z \in E]) \right) \\ &= \max_{x,y} \left(\sup_E (\Pr[x + Z \in E] - \Pr[y + Z \in E]) \right) \\ &= \max_{x,y} \text{TV}(X + Z|X = x, Y + Z|Y = y) \end{aligned}$$

This concludes the proof. \square

Theorem 5.1 (Privacy amplification for the training dataset). *Suppose that the underlying training process of the black-box model f is $(\hat{\epsilon}, \hat{\delta})$ -differentially private w.r.t. the training dataset, then the explanation algorithm described in Algorithm 1 with parameters (ϵ, δ) is $(\hat{\epsilon}, \gamma\hat{\delta})$ -differentially private for the training dataset, where, $\gamma \in 1 - \mathcal{O}\left(\left(\frac{\log T}{m\epsilon}\right) \left(e^{-\frac{m\epsilon}{\log(T/\delta)}}\right)\right)$. Moreover for any training process, Algorithm 1 is $(\mathcal{O}(m\epsilon), \delta)$ -differentially private for the training dataset.*

Proof. We first bound the sensitivity of gradients with respect to the training dataset; i.e. if a particular datapoint is removed from the training dataset of the black-box model f , then the change in the gradient of the loss function is bounded given ϕ and explanation dataset \mathcal{X} . Suppose that f and f' are black-box models trained on the training set \mathcal{T} and $\mathcal{T} \setminus \vec{v}$ respectively; then for any $\phi_1, \phi_2 \in \mathcal{C}_{2,1}$, explanation dataset \mathcal{X} and weight function $\alpha(\cdot) \in \mathcal{F}(c, \vec{z})$:

$$\begin{aligned}
& \|\nabla\mathcal{L}(\phi_1, \mathcal{X}, f) - \nabla\mathcal{L}(\phi_2, \mathcal{X}, f')\| \\
&= \frac{2}{m} \left\| \sum_{\vec{y} \in \mathcal{X}} \alpha(\|\vec{y} - \vec{z}\|) ((\phi_1 - \phi_2)^\top (\vec{y} - \vec{x}) + f(\vec{y}) - f'(\vec{y})) (\vec{y} - \vec{z}) \right\| \\
&\leq \frac{c}{m} \sum_{\vec{y} \in \mathcal{X}} \frac{(|f(\vec{y}) - f'(\vec{y})|) + (\|\phi_1\| + \|\phi_2\|) \|\vec{y} - \vec{z}\|}{(1 + \|\vec{y} - \vec{z}\|)} \leq 2c
\end{aligned} \tag{13}$$

The first inequality is derived from the fact that $\alpha(\cdot) \in \mathcal{F}(c, \vec{z})$. Let $\mathcal{M}(\mathcal{T})$ and be the training process on the dataset \mathcal{T} which outputs a probability distribution on the parameter space of the black-box model Θ where each θ corresponds to the learned black-box function. For a fixed parameter $\theta \in \Theta$ (black-box function f), our explanation algorithm computes T many noisy iterative gradients $\mathcal{L}(\vec{x}, \phi^{\{i\}}, f) + Z$ for $i = 0, \dots, T-1$ and output $\phi^{\{T\}}$, a probability distribution over explanations (set \mathcal{C}). To show that this transformation³ improves the privacy guarantees of the training dataset due to randomness added during the optimization, we use similar techniques described in [8], and utilize contraction transformations.

Now, for any two different parameterizations $\theta_1, \theta_2 \in \Theta$, we denote the corresponding black-box functions f_1, f_2 . For simplicity, we denote the distribution of $\phi^{\{T-1\}} - \eta(T-1)\nabla\mathcal{L}(\phi^{\{T-1\}}, f)$ as μ . The total variation between the distribution $\phi^{\{T\}}|\theta_1, \phi^{\{T\}}|\theta_2$ can be written as:

$$\begin{aligned}
& \text{TV}(\phi^{\{T\}}|\theta_1, \phi^{\{T\}}|\theta_2) = \text{TV}(\mu + \eta(T-1)Z_{T-1}|\theta_1, \mu + \eta(T-1)Z_{T-1}|\theta_2); Z \sim \mathcal{N}(0, \sigma^2\mathbf{I}) \\
& \leq \max_{\phi_1, \phi_2 \in \mathcal{C}} \text{TV}(\mu + Z_{T-1}|\theta_1 \wedge \phi^{\{T-1\}} = \phi_1, \mu + Z_{T-1}|\theta_2 \wedge \phi^{\{T-1\}} = \phi_2)
\end{aligned} \tag{14}$$

Equation 14 follows from the Lemma H.1. Once we condition on $\phi^{\{T-1\}}$, both distributions in the above equation follows a Normal distribution with different means; we write $\phi_1 = \mu | \phi^{\{T-1\}}$ and $\phi_2 = \mu | \phi^{\{T-1\}}$ respectively. Both have the same variance: $\eta(T-1)^2\sigma^2\mathbf{I}$. Note that ϕ_1 and ϕ_2 are not random quantities. For Gaussian random variables with same variance matrix and different means, [9, Theorem-1], provides the exact value of the total variation distance between

³More formally we can define the transformation as a Markov kernel. For more details, see [8]

them. Using this result we obtain:

$$\begin{aligned}
& \text{TV}(\phi^{\{T\}}|\theta_1, \phi^{\{T\}}|\theta_2) & (15) \\
& \leq \max_{\phi_1, \phi_2 \in \mathcal{C}} 2 \Pr \left[Z \in \left(0, \frac{\|\phi_1 - \phi_2 + \eta(T-1)(\nabla \mathcal{L}(\phi_2, f_1) - \nabla \mathcal{L}(\phi_2, f_2))\|}{2\eta(T-1)\sigma} \right) \right] \\
& \leq \max_{\phi_1, \phi_2 \in \mathcal{C}} 2 \Pr \left[Z \in \left(0, \frac{\|\phi_1\| + \|\phi_2\| + \eta(T-1)\|\nabla \mathcal{L}(\phi_2, f_1) - \nabla \mathcal{L}(\phi_2, f_2)\|}{2\eta(T-1)\sigma} \right) \right] \\
& \leq \max_{\phi_1, \phi_2 \in \mathcal{C}} 2 \Pr \left[Z \in \left(0, \frac{1 + \eta(T-1)c}{\eta(T-1)\sigma} \right) \right] = 2 \Pr \left[Z \in \left(0, \frac{1 + \eta(T-1)c}{\eta(T-1)\sigma} \right) \right] \\
& \leq 2 \Pr \left[Z \in \left(0, \frac{m\epsilon}{16\sqrt{2} \log\left(\frac{2T}{\delta}\right)} \right) \right] & (16)
\end{aligned}$$

Where $Z \sim \mathcal{N}(0, 1)$. The first inequality in Equation 16 follows from Equation 13. Equation 16 and [8, Theorem 1] concludes the proof of the first part of the theorem.

The second part follows from Equation 13. The sensitivity of the gradient wrt. training dataset is $2m$ times the sensitivity of the explanation dataset. Concluding the proof. \square